THESIS APPROVAL

GRADUATE SCHOOL, KASETSART UNIVERSITY

Master of Engineering (Information and Communication Technology for Embedded Systems)
DEGREE

Information and Communication Technology for Embedded Systems
FIELD

Electrical Engineering
DEPARTMENT

TITLE: Hand Motor Imagery EEG Classification Using Adaptive Band Selection for Brain-Computer Interface

NAME: Mr. Payat Jirasuwanpong

THIS THESIS HAS BEEN ACCEPTED BY

.....
THESIS ADVISOR

(Mr. Miti Ruchanurucks, Ph,D.)

.....
THESIS CO-ADVISOR

(Mr. Chusak Thanawattano, Ph,D.)

.....
THESIS CO-ADVISOR

(Associate Professor Nobuhiko Sugino, Dr.E.)

.....
DEPARTMENT HEAD

(Assistant Professor Teerasit Kasetkasem, Ph.D.)

APPROVED BY THE GRADUATE SCHOOL ON .....

.....
DEAN

(Associate Professor Gunjana Theeragool, D.Agr.)

THESIS

HAND MOTOR IMAGERY EEG CLASSIFICATION USING ADAPTIVE BAND SELECTION FOR BRAIN-COMPUTER INTERFACE

PAYAT JIRASUWANPONG

A Thesis Submitted in Partial Fulfillment of
the Requirements for the Degree of
Master of Engineering (Information and Communication Technology for Embedded Systems)
Graduate School, Kasetsart University
2011

Payat Jirasuwanpong 2011: Hand Motor Imagery EEG Classification Using Adaptive Band Selection for Brain-Computer Interface. Master of Engineering (Information and Communication Technology for Embedded Systems), Major Field: Information and Communication Technology for Embedded Systems, Department of Electrical Engineering. Thesis Advisor: Mr. Miti Ruchanurucks, Ph.D. 78 pages.

Brain-Computer Interface (BCI) is a system designed for a specific application. In hand motor imagery, the Electroencephalograph (EEG) signal related to motor activity can be recorded from the sensorrimotor area, which releases informative signals during motor execution. Patterns used to classify left and right hand motor imagery are called Event Related Desynchronization (ERD). However, an individual produces the informative patterns in different frequency components. Therefore, the BCI system needs to be appropriately designed for both applications and subjects. This thesis attempts to design an adaptive filter for selecting proper frequency bands of each person. The filter based on wavelet transform is called Wavelet Filter. Nevertheless, the wavelet filter will not be adaptive if there is no band selection. The band selection is to choose the most discriminative bands by using a cost function. When a value from a cost function is high, it means there is high discrimination between the patterns of the two classes. After the process selects the bands, the adaptive wavelet filter will be implemented to eliminate undesirable components. In summary, the results indicate that the proposed method achieves higher classification accuracy than that of static filters.

_____ _____ __ / __ / __

Student's signature Thesis Advisor's signature

ACKNOWLEDGEMENTS

This research is financially supported by Thailand Advanced Institute of Science and Technology - Tokyo Institute of Technology (TAIST-Tokyo Tech), National Science and Technology Development Agency (NSTDA), Tokyo Institute of Technology (Tokyo Tech) and Kasetsart University (KU).

Officially, I would like to thank Mr. Miti Ruchanurucks, thesis advisor, for motivating me to be an avid learner, suggesting the direction of the thesis, sharing his experiences, and indispensably giving souvenirs from many countries. I would like to thank Dr. Chusak Thanawattano, thesis co-advisor from NECTEC, to give basic information of biomedical signal and suggestion about scope of the thesis. I appreciate Prof. Nobuhiko Sugino, thesis co-advisor from Tokyo Institute of Technology, to give valuable comments about hardware and software, and it's kind of him to bring gifts to his students every time he met. In my related work, I want to thank Mr. Samatcha and Mr. Yassine, bachelor's degree students in our lab, to let me know about some characteristics of recording hardware.

Personally, this thesis gains a lot of convenience from Miss. Pornpawee, secretary of the ICTES program; thus, I would like to thank her here also. Many friends that give interesting discussions about this thesis are not mentioned here, so I want to thank them all. Finally, I really would like to thank my family for ambition, good comments, and crucially unequivocal supports.

Payat Jirasuwanpong

June 2011

TABLE OF CONTENTS

Page

LIST OF TABLES

LIST OF FIGURES

LIST OF FIGURES (Continued)

LIST OF ABBREVIATIONS

BCIs	=	Brain-Computer Interface system
EEG	=	Electroencephalogram
ERD	=	Event Related Desynchornization
ERS	=	Event Related Synchornization
STFT	=	Short Time Fourier Transform
WT	=	Wavelet Transform
WD	=	Wavelet Decomposition
WPT	=	Wavelet Packet Transform
WPD	=	Wavelet Packet Decomposition
DWT	=	Discrete Wavelet Transform
LDB	=	Local Dicriminant Bases
CSP	=	Common Spatial Pattern
LDA	=	Linear Discrimination Analysis
LSVM	=	Linear Support Vector Machine
SVM	=	Support Vector Machine
ANN	=	Artificial Neural Network
HMM	=	Hidden Markov Model
CAR	=	Common Average Referenced
FIR	=	Finite Impulse Response

HAND MOTOR IMAGERY EEG CLASSIFICATION USING ADAPTIVE BAND SELECTION FOR BRAIN-COMPUTER INTERFACE

INTRODUCTION

Brain-Computer Interface systems (BCIs) are a machine that translates brain waves into commands. The interaction between a human brain and computers provides an alternative channel for paralyzed patients not only in the field of rehabilitation but also in the field of communication. Nowadays, researchers are working hard at the crossroad of computer science, neurosciences, and biomedical engineering. The system is comprised of a device recording neural signals, an effecter controlled by commands, and an algorithm interpreting the signal into instructions.

First of all, Electroencephalogram (EEG) signal is widely used in a non-invasive system, and EEG recording devices are divided into 2 parts: analog part and digital part. The analog part consists of sensors, amplifiers, and active filters. Brain signal is recorded by sensors called electrodes. Although there are many types of the electrode, researchers have tendency to use Ag-AgCl electrodes because it's reasonable between cost and quality. As electrodes are necessary to be placed on suitable positions, an EEG cap, which electrodes are installed on, is provided for precise measurement the neural signal. The widely-used standard of the EEG cap is the 10-20 system. The 10-20 system is based on distance between locations of electrodes and underlying areas of cerebral cortex. Owning to small amplitudes and noisy measurements of EEG signal, the signal must be passed through an amplifier in order to change level of the signal from micro voltage to voltage. In addition, irrelevant frequency components can be eliminated by active band-pass filters. The active filter implemented by operational amplifier (op-amp) consumes electric power; therefore, it is called active filters. The filter not only eliminates undesirable components but can gain amplitudes in the range of filter designation also. Another part is the digital part that consists of analog-to-digital convertors, FIR filters, and

Notch filters. To change analog signals into digital signals, we use an analog-to-digital convertor (A/D). Normally, EEG signal is digitized at 16 bit resolution and sampled at 256 Hz. After quantization from analog to digital, the signal needs filtering by digital filters. Even though, the signal was passed through the analog filter, it is essential to filter the signal again. An analog filter is basically used to amplify amplitudes in a pass-band range but not is used to eliminate undesirable components. Therefore, the digital filter operates in decreasing noisy components. Besides, Notch filters are employed in reducing electric noise from 50 Hz power lines (50 Hz in Thailand). Subsequently, the operated signal is stored in a computer in order to process both offline and online application further.

The second is an effecter controlled by commands. We need to know all physical characteristics of the effecter in order to model it into mathematic equations. Subsequently, it can be controlled by electrical instructions. For example, if the system is used to control a robot arm, the robot arm must be measure length, width, and distance in order to built characteristic equations first. EEG signal is decided into instructions that are used as parameters of the equations to change output of the effecter.

The most important module of the BCI system is an algorithm that relies on methodologies. Methods of the system based on signal processing consist of preprocessing, enhancement, feature extraction, and classification. First, because EEG signal is contaminated by interference waveforms called artifacts, and types of EEG signal depend on a frequency range, EEG signal need selecting the range of interest. The selection is to suppress artifacts and retain essential patterns. Furthermore, because the informative pattern emerges in diverse time, for enhancement, Time-Frequency analysis is used in selecting appropriate time duration and informative bands in order to clarify the pattern. Feature extraction is a method that finds some characteristics to represent the signal. Features have a highly impact on classification accuracy. The BCI system has wildly used effective features to represent EEG signal, such as statistical model, probabilistic model, power spectrum, and energy. A

classifier which is a learning machine trained by features will recognize the patterns. Then, it will decide patterns in order to turn brain waves into an instruction.

In conclusion, a good BCI system must consist of three important modules: recording devices that measure brain activity in relative positions, An effecter controlled by the related signal for several applications, and an algorithm that is a method of the translation signals into commands. The process must appropriately choose a method for classification accuracy. Finally, the BCI systems will be designed for a specific task. Therefore, we need develop a proper way to deal with a suitable application.

Motivation

The BCI system focuses on offering a human-interacting channel not only medical applications but also psychology study. The system is used in medical applications which must be in the control of a doctor. The more we have a variety of diagnosis, the more accurate a doctor can analyze diseases. The brain interface provides easy ways for a doctor to access patient's brain by using computers. This communication is suitable for paralytics to receive appropriate treatment. Even through paralytics cannot move their limbs, their brains are still able to respond as normal. For example, a paralytic will be able to communicate with other people by thinking that makes him can ask for his requirement and state his symptom. In addition, not only is the BCI system used in medical analysis but also it can be applied to diverse fields. A psychology field directly related to brains gains benefices from the BCI system as well. Because psychologists need to know responds of subjects during an action, they are able to analyze brain waves from the system. For instance, in sport, coaches can study world-class sportsman thinking.

Raw EEG signals need preprocessing to enhance precision of signal interpretation. First, each brain activity corresponding a specific frequency range occurs, while brains are being stimulated by an experiment task. Informative patterns emergence depends on stimulated time; therefore, it is called non-stationary signal,

which the signal contains both time and frequency information. We need to come up with the solution to a feature-mixed problem. One of the solutions is to use time-frequency analysis, such as Short Time Fourier Transform (STFT), Wavelet Transform (WT), and Wavelet Packet Transform (WPT). When the transforms extract time and frequency features, researchers will analyze the data precisely. In addition, raw EEG signal has a low signal-to-noise ratio resulting in ineffective interpretation. Thus, the raw signal need removing noise to gain a higher signal-to-noise ratio. Noise removal is employed to eliminate outlier while retaining significant information.

Brain response of the same action differs from person to person both activated areas and frequency components. While a brain is being stimulated by a task, related areas release informative brain wave. Thus researchers can install electrodes on these areas to measure brain activity. Unfortunately, the activated areas are not the same positions in each person. For example, during left hand moving, an activity on the right side of the motor area is occurred. However, there are many electrodes placed on this area. The highest-powered activity may take place on channel C_4 or other adjacent positions. Another notion is a variety of frequency components. A frequency range of activity depending on subject's anatomy is also specific for a person, but almost all individual ranges are covered in the average-experimented frequency range. For instance, MU band used in motor activity have an approximate range at 8-12 Hz, but an eminent frequency range of a subject may lie on 10-12 Hz. Thus, proper electrode positions and informative bands are chosen by adaptive processing for making the system suitable for an individual.

Medical Background

This medical background article derives from a part of fundamentals of "EEG Technology Volume 1: Basic Concept and Methods" book (Fay *et al.,* 1983) and additionally some information from the Internet.

1. Electroencephalogram (EEG) Signal

An electroencephalogram, abbreviated EEG, is a visible record of the amplified electrical activity generated by the nerve cells of the brain. The electrical activity can be recorded through the skull by placing electrodes on the scalp. As you can see, rising and falling electrical potentials are called brain waves. The sources of electrical activity are in the millions of nerve cells called Neurons, which compose the brain substance. In recording nerve response, a small area under each electrode is on the cortex, which is the outer surface of the brain. The synchronously changing in many neurons results in rhythms of various types describing below (http://en.wikipedia.org/wiki/Electroencephalography).

Delta is the frequency range up to 4 Hz shown in Figure 1. It tends to be the highest in amplitude and the slowest waves. It is seen normally in adults in slow wave sleep. It is also seen normally in babies. It may occur focally with subcortical lesions and in general distribution with diffuse lesions, metabolic encephalopathy hydrocephalus or deep midline lesions. It is usually most prominent frontally in adults (e.g. FIRDA - Frontal Intermittent Rhythmic Delta) and posteriorly in children (e.g. OIRDA - Occipital Intermittent Rhythmic Delta).

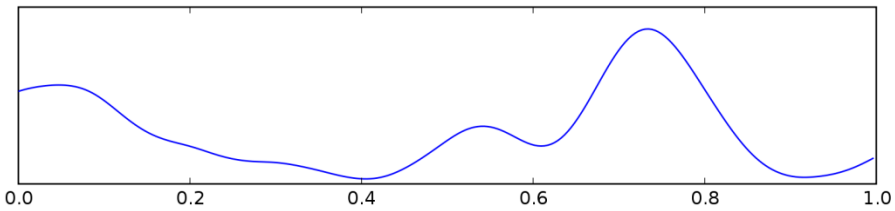

Figure 1 The Delta rhythm of EEG signal.

Theta is the frequency range from 4 Hz to 7 Hz shown in Figure 2. Theta is seen normally in young children. It may be seen in drowsiness or arousal in older children and adults; it can also be seen in meditation. Excess theta for age represents abnormal activity. It can be seen as a focal disturbance in focal subcortical lesions; it can be seen in generalized distribution in diffuse disorder or metabolic encephalopathy or deep midline disorders or some instances of hydrocephalus. On the contrary this range has been associated with reports of relaxed, meditative, and creative states.

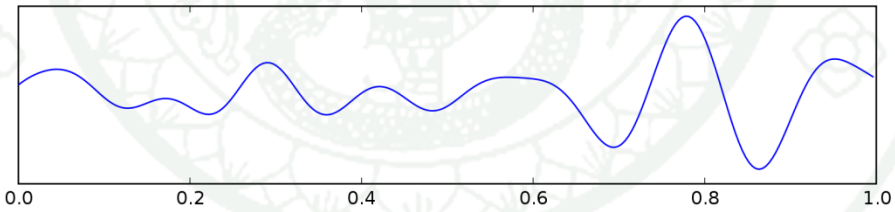

Figure 2 The Theta rhythm of EEG signal.

Alpha is the frequency range from 8 Hz to 12 Hz shown in Figure 3. Hans Berger named the first rhythmic EEG activity he saw as the "alpha wave". This was the "posterior basic rhythm" (also called the "posterior dominant rhythm" or the "posterior alpha rhythm"), seen in the posterior regions of the head on both sides, higher in amplitude on the dominant side. It emerges with closing of the eyes and with relaxation, and attenuates with eye opening or mental exertion. The posterior basic rhythm is actually slower than 8 Hz in young children (therefore technically in the theta range). In addition to the posterior basic rhythm, there are other normal alpha

rhythms such as the MU rhythm (alpha activity in the contralateral sensory and motor cortical areas that emerges when the hands and arms are idle; and the "third rhythm" (alpha activity in the temporal or frontal lobes). Alpha can be abnormal; for example, an EEG that has diffuse alpha occurring in coma and is not responsive to external stimuli is referred to as "alpha coma".

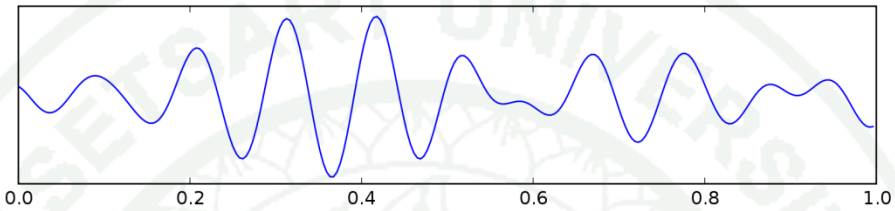

Figure 3 The Alpha rhythm of EEG signal.

Beta is the frequency range from 12 Hz to about 30 Hz shown in Figure 4. It is seen usually on both sides in symmetrical distribution and is most evident frontally. Beta activity is closely linked to motor behavior and is generally attenuated during active movements. Low amplitude beta with multiple and varying frequencies is often associated with active, busy or anxious thinking and active concentration. Rhythmic beta with a dominant set of frequencies is associated with various pathologies and drug effects, especially benzodiazepines. It may be absent or reduced in areas of cortical damage. It is the dominant rhythm in patients who are alert or anxious or who have their eyes open.

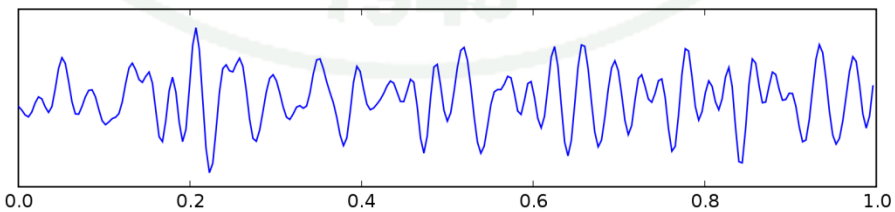

Figure 4 The Beta rhythm of EEG signal.

Gamma is the frequency range approximately 30–100 Hz shown in Figure 5. Gamma rhythms are thought to represent binding of different populations of neurons together into a network for the purpose of carrying out a certain cognitive or motor function.

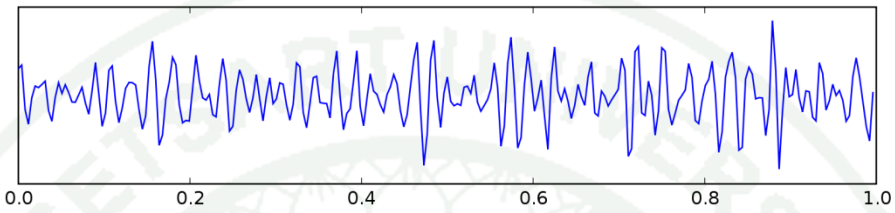

Figure 5 The Gamma rhythm of EEG signal.

Mu ranges 8–13 Hz shown in Figure 6, and partly overlaps with other frequencies. It reflects the synchronous firing of motor neurons in rest state. Mu suppression is thought to reflect motor mirror neuron systems, because when an action is observed, the pattern extinguishes, possibly because of the normal neuronal system and the mirror neuron system "go out of sync", and interfere with each other.

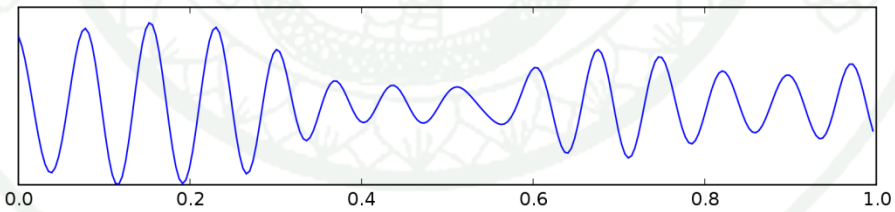

Figure 6 The Mu rhythm of EEG signal.

2. Electrode

EEG electrodes are the first instrumental link between the electrical generators in the brain. EEG electrodes are pieces of metal held against the scalp with a conductive jelly beneath them and wired to inputs of EEG amplifiers. The events

that occur at the interface of the electrode and the jelly called an electrolyte shown in Figure 7 are great importance because at this interface, current flow within body becomes electron flow in the electrode. The formation of two closely spaced and opposing charges is equivalent to the plates of a charged capacitor. Consequently, an EEG electrode placed on the scalp has the property of a capacitor. Different metals develop different voltages when immersed in the same electrolyte. Generally, EEG electrodes have two material components by using one electrode material as a standard. This electrode is called half-cell potential because single electrode acts as half of a battery. Therefore, two materials are used in the construction of electrodes in order that electrodes have the property of a battery. The equivalent circuit of the electrodes including electrolyte interface is shown in Figure 8.

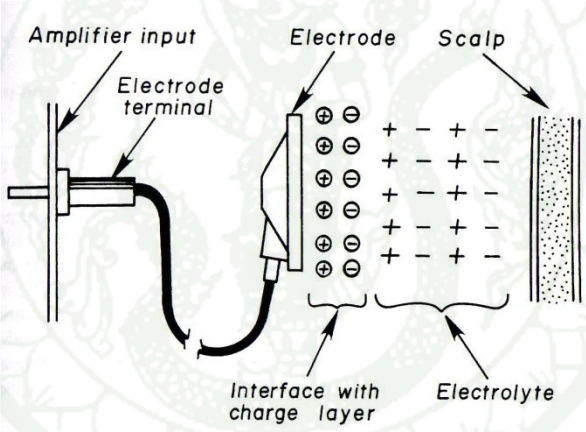

Figure 7 Electrode installation and the function of electrolyte.

Source: Fay *et al.,* (1983).

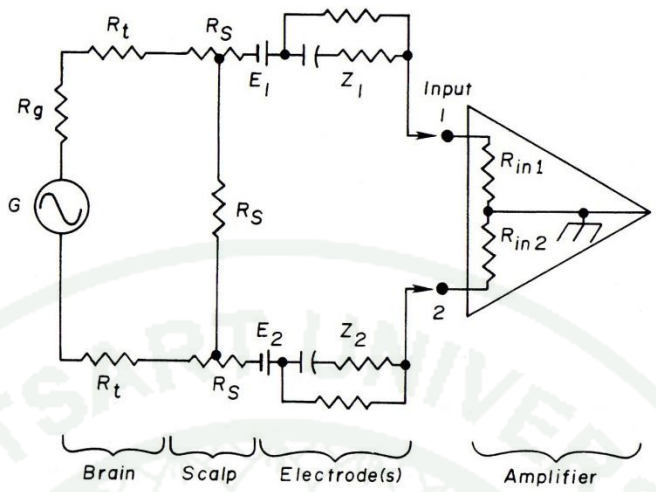

Figure 8 Equivalent circuit of an electrode.

Source: Fay *et al.,* (1983).

Capacity and resistive elements result in electrode impedance. The impedance of each electrode should be equal in order that DC voltage appearing at inputs also will be equal. Because of the property of the capacity, electrodes have properties of high-pass filter and a time constant. In general, electrodes present high impedances to very low frequency signals and low impedances to higher frequency signals. Empirical evidence suggests silver-silver chloride electrode is the best not only minimum drift of electrode potential but also a very time constant.

2.1 Surface Electrode

Surface electrodes are metal discs or shallow cups, and the diameter may vary from 4 to 10 mm. Most of the cup electrodes have a hole in their center through which the electrolyte can be introduced after attachment to the scalp. Before surface electrodes are applied, the scalp must be prepared properly, requiring topical cleaning at the measured locations. Local scrubbing with a gauze pad using alcohol will remove local oils and reduce scalp resistance. After the local area is cleaned, an electrolyte, usually an ECG paste containing free chloride ions, is rubbed into it. A

small amount of electrolyte is then speared on the surface of the electrode to be placed against the scalp, and a cup electrode is filled with electrolyte. The most effective method of securing an EEG electrode to the scalp is to use an EEG cap as Figure 9. EEG caps are used to hold the electrodes in place to the subject's head during routine EEG tests. With the help of the grid (created by the longitudinal and lateral silicon tubes), the electrodes can be placed on the patient's head and held in place. This is done according to the International 10-20 electrodes placement system. There are general two types of EEG caps: Standard and Universal caps. Standard caps are designed for a quick application, and they are offered in different sizes but they are unable to resize. Universal caps have a tube grid that is able to resize totally in any direction. So it is possible to adapt the cap size individual to the patients head.

Figure 9 An EEG cap in the 10-20 system.

Source: JNetDirect Biosciences (2008).

2.2 Measurement of Electrode Impedance

Regardless of electrode types, the impedance (Z) of every electrode should be measured before recording begins. This measurement is carried out by using an AC impedance meter. Generally, the impedance of subdermal electrodes is higher than the impedance of surface electrode limited by surface area. For example,

an effective subdermal electrode with a diameter of 12 mm has a surface area of 20 mm^2 while the surface area of a 10-mm disc electrode is 78.5 mm^2. The impedance of most electrodes varies with the frequency of the recorded signal, particularly below 10 Hz. The impedance of Ag-AgCl surface electrode remains constantly low from 10 Hz to less than 1 Hz. Others confirm the poor impedance of subdermal electrode at low frequencies, especially below 0.5 Hz. The use of a DC ohmmeter can determine only resistance, but it does not include any capacitive component. Therefore, the use of AC impedance meters has been implemented to measure the impedance by using a 10 to 30 Hz alternatively current (EEG frequency range). Electrode impedance meters may be connected directly to board of the EEG for expedient measurement. All electrodes expect the tested one are interconnect within the device, and then the impedance of the selected electrode is measured against the impedance of the other in parallel. A switch consecutively selects electrodes should be below 5 kΩ. After a recording has started, it's necessary from time to time to recheck the impedances, particularly if there are unusual asymmetries. Many modern EEG instrument have a built-in impedance checking system. If an electrode's impedance rises above 5 kΩ, it should be reduced by adding electrolyte, or the electrode should be replaced as necessary.

3. Electrode Placement

An EEG recording system can be facilitated if there are general agreements regarding the locations of the electrodes. The system of electrode placement was called "ten-twenty electrode system", and it is widely used throughout the world. The basic principles endorsed by the America Electroencephalographic Society are that Positions of electrodes should be determined by measurement from standard landmarks on the skull. Measurement should be proportional to skull size and shape, insofar as possible. Adequate coverage of all parts of the head should be provided with standard designated positions. Designation of positions should be in terms of brain areas (Frontal, Parietal, etc.) rather than only in numbers, so that communication becomes more meaningful. Anatomical studies should be carried out to determine the

cortical areas more likely to be found beneath each of the standard electrode positions in the average subject.

The locations of the electrodes are shown in Figure 10. Each electrode has a standard abbreviation based on the brain area it represents. Odd-numbered positions are on the left and even-numbered positions are on the right.

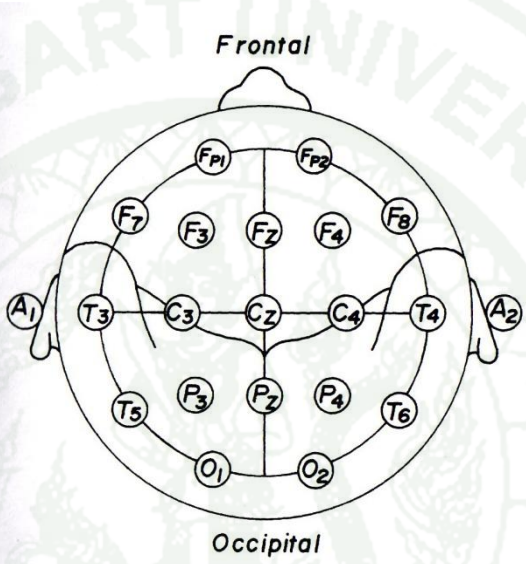

Figure 10 Electrode placement of the 10-20 system.

Source: Fay *et al.,* (1983).

The landmark anatomical points referred to by the Committee are shown in Figure 11 consisting of nasion, inion, left and right preauricular points. By proceeding from these four landmarks, it is possible to establish locations for all of the electrode placements shown in Figure 10.

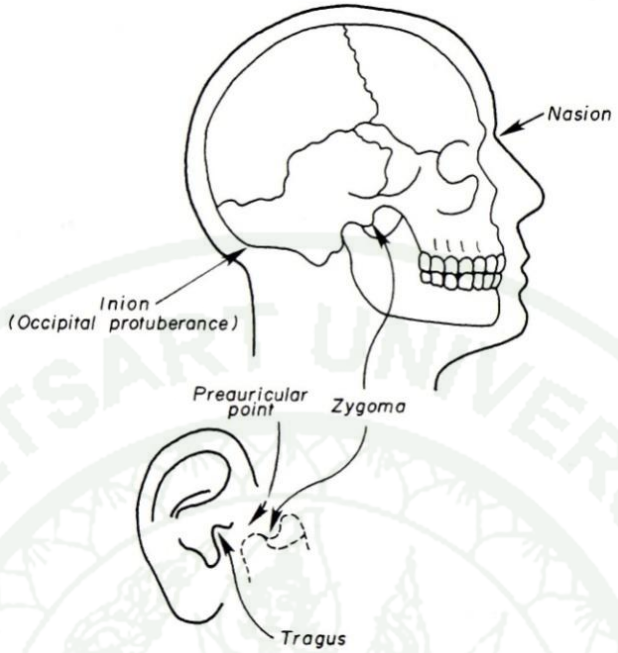

Figure 11 Anatomical landmarks.

Source: Fay *et al.*, (1983).

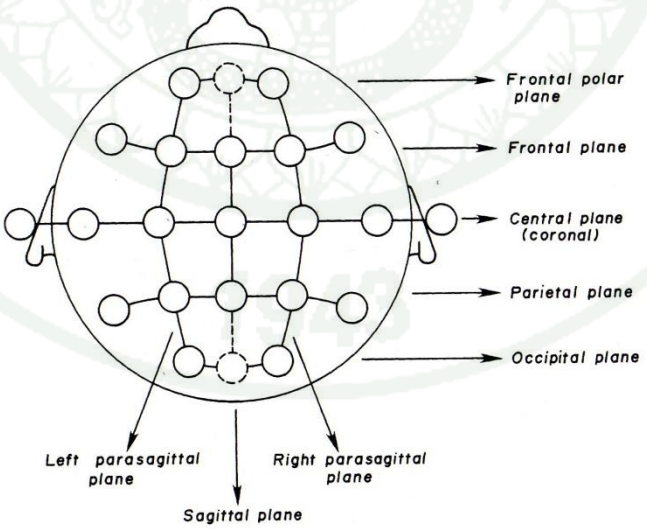

Figure 12 Anteroposterior and transverse planes.

Source: Fay *et al.*, (1983).

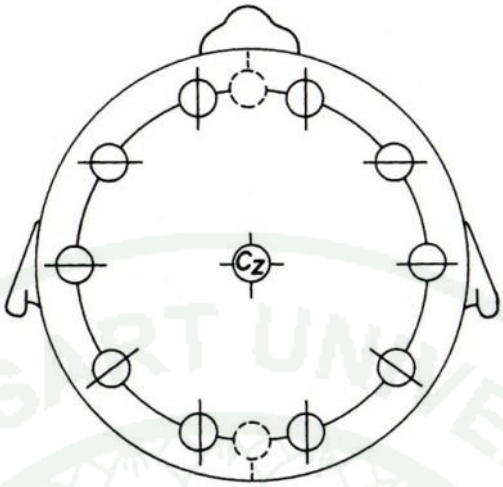

Figure 13 Circumferential plane.

Source: Fay *et al.,* (1983).

In Figure 12, the electrodes have been organized by front-to-back lines and left-to-right lines. front-to-back lines are identified as the left anteroposterior, the sagittal (which is in the midline), and the right anteroposterior. The transverse lines are identified ordering from front to back as the frontal polar, the frontal, the central, the parietal, and the occipital. Another lines identified is a circumferential line above the preauricular points as Figure 13.

4. Polarity and Localization

The amplifier used for EEG recording is differential amplifiers. Each electrode is a recording of the difference in voltage between the electrode terminal 1 and the electrode terminal 2. If there is no difference in voltage at the input terminals, the output will be zero. All EEG instruments, by international agreement, are designed so that input 1 more negative than input 2, the wave rises up in an upward direction. Further, when input 2 is more negative then input1, the wave declines in a downward direction. On the other hands, when input 1 is more positive than input 2,

the wave moves in a downward direction, and when input 2 is more positive, the wave also moves in an upward direction.

4.1 Bipolar Recording

Bipolar recording uses multiple electrode derivations (a derivation is a pair of electrodes) without any one common electrode connected with input of all the channels. Usually, the derivations are arranged so that the electrodes are in a straight line called an array, and adjacent channels have an electrode in common as shown in Figure 14. The shared electrode (C_3) results in activity localization. For example, when a negative event occurs near electrode C_3, channel 1 has a downing movement and upgoing movement at channel 2. In contract, if the event becomes positive, the first channel has an upgoing, while the second channel has a downing.

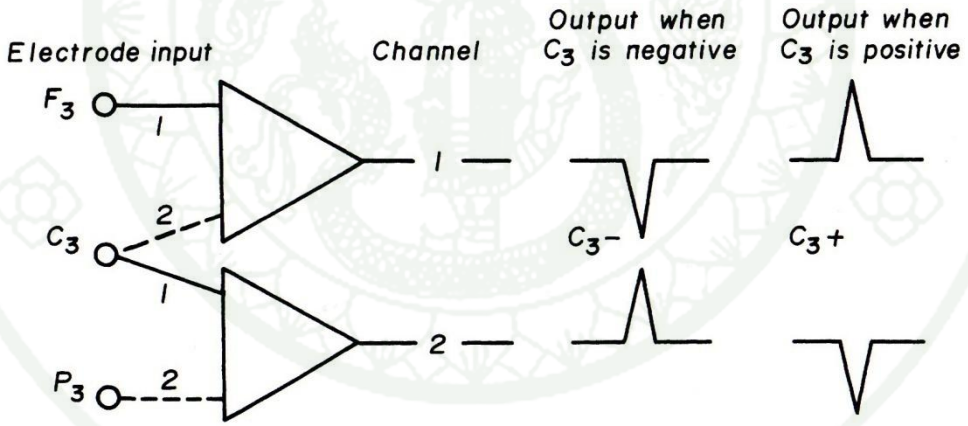

Figure 14 Two-channel bipolar recording.

Source: Fay *et al.*, (1983).

4.2 Reference Recording

Reference recording (sometimes called monopolar) of the same EEG event would require three amplifiers as shown in Figure 15. A different scalp

electrode is connected to input 1 of each amplifier, and a single common reference electrode is connected to input 2 of each amplifier. Normally, the left earlobe (A_1) is used as the reference (R). If a negative EEG event occurs at C_3, it will produce an upward movement in channel 2, whereas other channels show no charge. On the other hands, if a positive event occurs, the output of channel 2 will move downwardly, and others also show no charge.

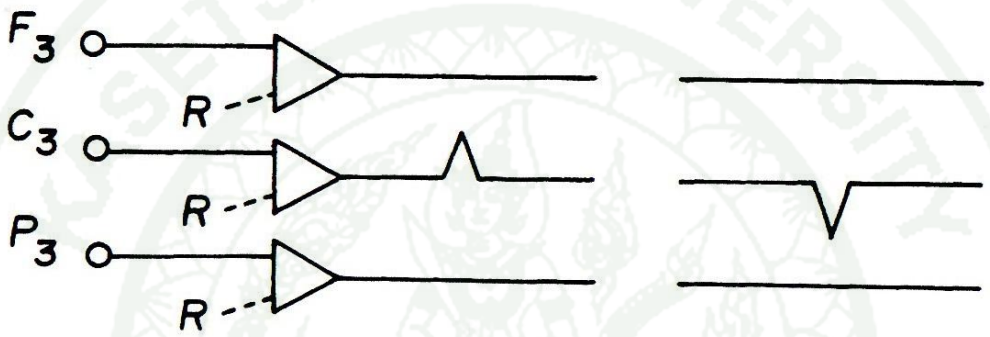

Figure 15 Referential recording.

Source: Fay *et al.*, (1983).

4.3 Fields

Transient focal EEG activities that are negative at the surface of the scalp are called surface negative events. By using either bipolar or referential surface derivations, it is possible to localize an EEG event to either a small or a large area of the scalp called a field. The field can be described in terms of its surface polarity shown in Figure 16.

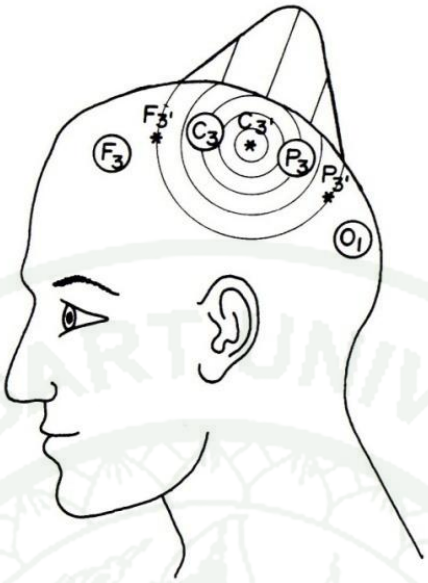

Figure 16 Field of brain activity.

Source: Fay *et al.,* (1983).

In Figure 16, it shows the equipotential area, in which the voltage is equal, on C_3 and P_3. However, it is feasible that there may be a higher or a lower potential between these locations. This problem can be solved by adding more electrodes located between older electrodes to an array. The circle line inside the field is an equipotential line. As you see in Figure 16, C_3 and P_3 were not at the focal point, and the field can be drawn schematically on the scalp as in Figure 17. A reference recording of the event is displayed in Figure18.

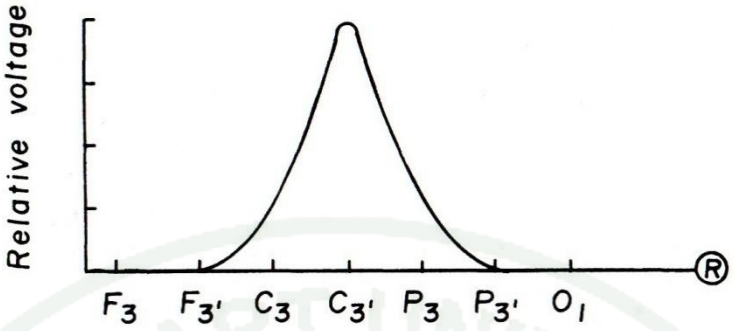

Figure 17 Graph representation of the field.

Source: Fay *et al.,* (1983).

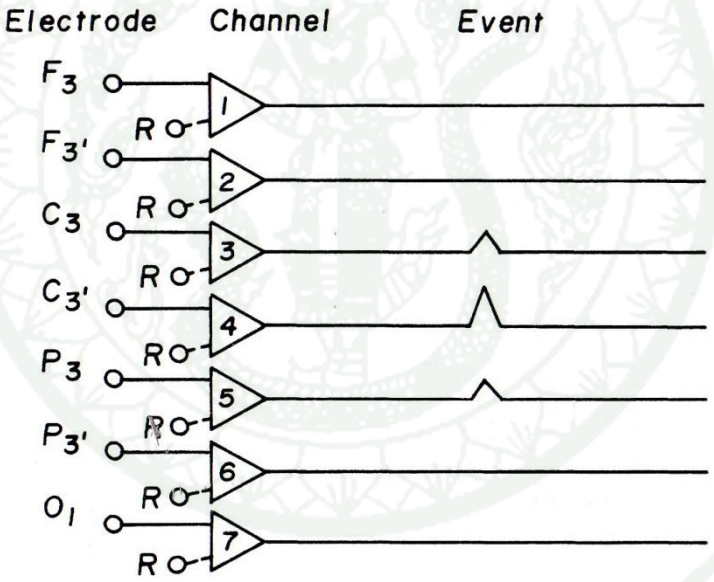

Figure 18 Referential recording in the same event.

Source: Fay *et al.,* (1983).

4.4 Contaminated Reference

In Figure 19, it shows a reference-contaminated situation. A focus is presented at T_3, the left midtemporal area, with a wide field surrounding it, extending as far as F_7 and A_1. The voltage at A_1 is less than that at T_3 and equal to the voltage at F_7. A reference recording is obtained with A_1 as the reference. Therefore, the reference (A_1) is contaminated by activity emerging at T_3. As you can see in Figure 20, 6 channels (Fp_1, T_5, F_3, C_3, P_3, and O_1) have a downward deflection, one channel (T_3) has a small upward deflection, and one channel (F_7) has no deflection. Because A_1 is common to all channels connecting to input 2 of all channels, these deflections can be explained in the following manner: T_3 is slightly more negative than A_1. T_3 goes to input 1, causing an upward deflection. A_1 is more negative than Fp_1, T_5, F_3, C_3, P_3, and O_1. Because A_1 is on input 2, there is a downward deflection in all channels to which input 1 is connected to those electrodes. F_7 and A_1 are equipotential.

Figure 19 Schema of field relative to electrodes.

Source: Fay *et al.*, (1983).

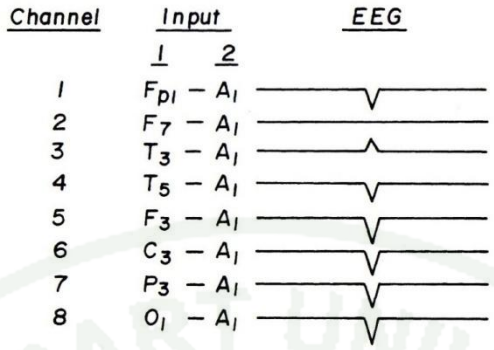

Figure 20 Output of each designed channels when using A_1 as reference.

Source: Fay *et al.*, (1983).

Such involvement of a reference electrode is not uncommon. It is sometimes called a contaminated reference. Based on understanding of the polarity rules, it will warn researchers to recognize the signs as illustrated in Figure 20. The contaminated reference problem can fix by changing the reference from A_1 to A_2 as shown in Figure 21.

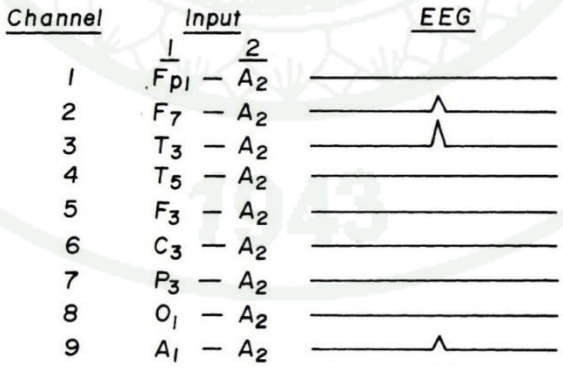

Figure 21 Output of each designed channels when using A_2 as reference.

Source: Fay *et al.*, (1983).

5. Artifacts

The EEG record is presumed to represent only cerebral activity. In reality, it includes undesirable electrical activities that deteriorate the brain signal. These noise activities are called artifact. Artifacts are divided into 2 types namely Physiological Artifact and Nonphysiological Artifact. Figure 22 shows the EEG record that combines artifacts.

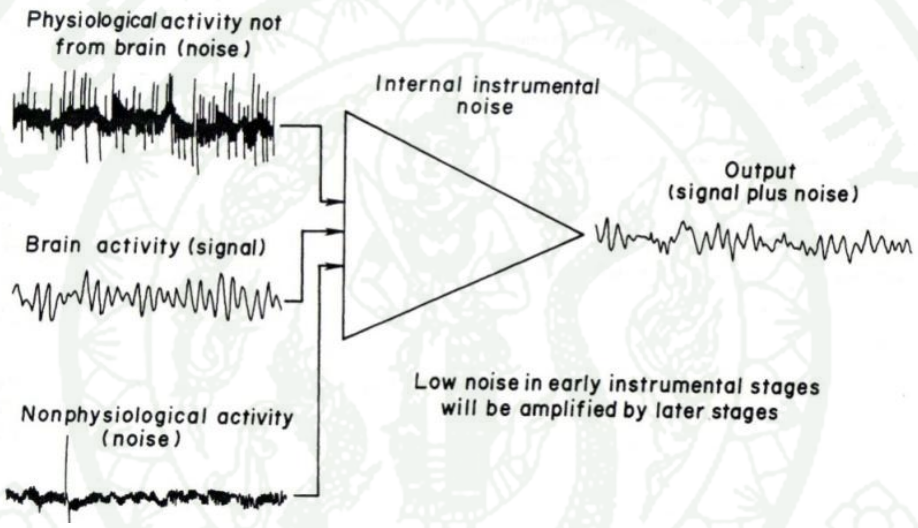

Figure 22 Noise from several sources.

Source: Fay *et al.*, (1983).

5.1 Physiological Artifact

Physiological artifact is electrical signals originating from other sources of the patient. These include muscle potentials, electrocardiographic potentials, potentials from the eyes, skin potentials, and glossokinetic potentials.

5.2 Nonphysiological Artifact

Nonphysiological artifact, which can be in the control of researchers, may originate from electrodes, switch contacts of the EEG instrument, or external signals.

5.2.1 50 Hz Artifact

50 Hz interference is the greatest nonphysiological noise in the EEG recording. There are two ways in which 50 Hz can produce the interference. The first is via electrostatic effects caused by capacitance between 50 Hz conductor (the AC mains wiring) and other conductor such as EEG electrode wires, metal bed frames, or the patient. Any capacitively-induced voltages reach the input of the EEG amplifiers. If the voltages at input 1 and input 2 are unequal, the output of the recording system will appear 50 Hz artifact. The second source of 50 Hz artifact is an electromagnetic effect, caused by electrical appliances such as transformers, power supplies in T.V., or EEG-associated equipment. The electrical field generated by these devices is inductively coupled to the electrode wires attached to the patient that act as the secondary of a transformer. Thus, 50 Hz interference will take place in the EEG recording. To eliminate 50 Hz artifact, the use of 50 Hz notch filters will remove all except very high voltage interference.

5.2.2 Artifacts Originating from Electrodes

A common artifact is electrode “pop”. This artifact may simulate a spike or sharp wave. It is caused by an electrically unstable electrode, by a drying electrolyte or by slight mechanical instability. On occasion, an electrode that has not been kept clean will develop pops and other electrical transients.

5.2.3 Internal Artifact

All amplifiers have internal noise. Internal noise is the result of electron moving randomly in the various parts of the amplifier as well as voltages created at all contact points in the circuit. Developers choose components with low inherent noise for using in their EEG amplifiers. The greatest source of noise is in the early stages of amplification before amplified progressively in later stages. If components in amplifiers fail, there may be an increase in noise beyond tolerable limits. Therefore, thorough study of manufacturer's instruction manual will help developers know the majority of problems.

OBJECTIVES

1. To classify EEG patterns of hand motor imagery between left and right.
2. To study impacts on EEG processing such as types of reference, kinds of filter, and the proposed method.
3. To design a specific filter for each user.

LITERATURE REVIEW

Classification of EEG patterns plays a key role in Brain-Computer Interface system (BCIs) especially non-invasive systems (Millá *et al.,* 2007; Stephan *et al.,* 2009). In hand motor imagery, patterns of brain oscillations reducing amplitudes of EEG signal is called Event-Related Desynchronization (ERD) used in classification. The oscillation has frequencies between 9-13 Hz corresponding to MU rhythm. Another activity related to motor imagery is Beta rhythm that lies on a frequency band at 16-24 Hz (Lopes *et al.,* 1857; Pfurtscheller *et al.,* 2006). Because of low signal-to-noise ratios and head volume contaminated EEG signals, Surface Laplacian Filtering have been a standard technique for removing artifacts and increasing signal-to-noise ratios (Oostendorp and Oosterom, 1996). In enhancement of EEG signals, initially, filter banks were applied to decompose the signal into subfrequency bands (Keng Ang *et al.,* 2008). However, the fixed bands require prior knowledge of reactive frequency bands. Therefore, an adaptive filter banks has been proposed to determine the most discriminative frequency bands by using Fisher ratio of spectral power (Kavitha *et al.,* 2009). Although the most discriminative bands were selected, the method did not consider features from multiple time and frequency indexes. Wavelet Transform (WT) has been used to consider the both features. WT implemented by band-pass filters is one of the Time-Frequency Analysis (Vetterli, 1992). Even though WT has had powerful efficiency to deal with non-stationary signals, the decomposed signals have a logarithmic frequency resolution. Wavelet Packet Transform (WPT), a developed version of WT, provides 2^{level} frequency resolutions to decompose EEG signal into subbands (Ting *et al.,* 2008). According to the perfect reconstruction property of the wavelet transform, a wavelet filter can be implemented by reconstructing only informative subbands of the decomposed signals (XiaoNan *et al.,* 2010). Nevertheless, features from subbands of WPT have high dimensionality. The large dimensional features influence not only on computation performance but classification accuracy also. Hence, Local Discriminant Bases (LDB) algorithm attempt to decrease redundancy of the subbands and increase the accuracy by find out an optimum tree (the best-basis paradigm). Furthermore, the most distinguished bands are proper bands (Saito and Coifman, 1995).

Feature extraction is a key issue in EEG classification. A great variety of features have been used to design BCIs, such as amplitude values of raw EEG signal (Kaper *et al.,* 2004), Power Spectral Density (PSD) (Millán and Mouriño, 2003), energy of wavelet coefficients (Bao GuoXu and Ai Guo, 2008), and Common Spatial Pattern (CSP) feature (Ramoser *et al.,* 2000). The feature selection must be considered properties of features following; noise and outliers, high dimensionality, time information, and small training set.

Several classifiers are used in BCIs. Such classifiers are roughly divided into two categories: linear classifiers and non-linear classifiers. Linear classifiers have a discriminating function that uses linear functions to distinguish classes. They are probably the most popular algorithms for BCIs like Linear Discrimination Analysis (LDA) (Pfurturtscheller, 1999), Linear Support Vector Machine (LSVM) (Schlögl *et al.,* 2005). On the other hand, non-linear classifiers that use more complicated functions are also used in BCI research because, in some cases, there are more accurate than linear classifiers. Non-linear classifiers perform more efficient rejection of uncertain samples, such as Artificial Neural Network (ANN) (Anderson and Sijercic, 1996), Support Vector Machine (SVM) (Kaper *et al.*, 2004), Bayes Decision Theory (Kolmorgen and Blanertz, 2002), and Hidden Markov Model (HMM) (Solhjoo *et al.*, 2005).

The Proposed Method

From an idea that we need to design an adaptive filter, we will design a specific filter for each person by selecting appropriate bands using energy of wavelet coefficients as a discriminative value. The selected bands will be a part of the designed filter implemented by a wavelet filter.

First of all, the signal of interest is decomposed into subbands by Wavelet Packet Decomposition (WPD). Every subband is calculated a discriminative value using energy coefficient of each band following band selection box in Figure 23. The subbands are sorted by descending order of the value, and we select the highest-valued bands. The wavelet filter is implemented by decomposing the signal into subbands. The filter is able to eliminate undesirable bands by remaining the selected bands from the previous process and adding zeros to the undesirable bands. Then, we reconstruct the selected signals using the perfect reconstruction property. The reconstructed signal is the band-pass filtered signal. The diagram below (Figure 23) shows the proposed method.

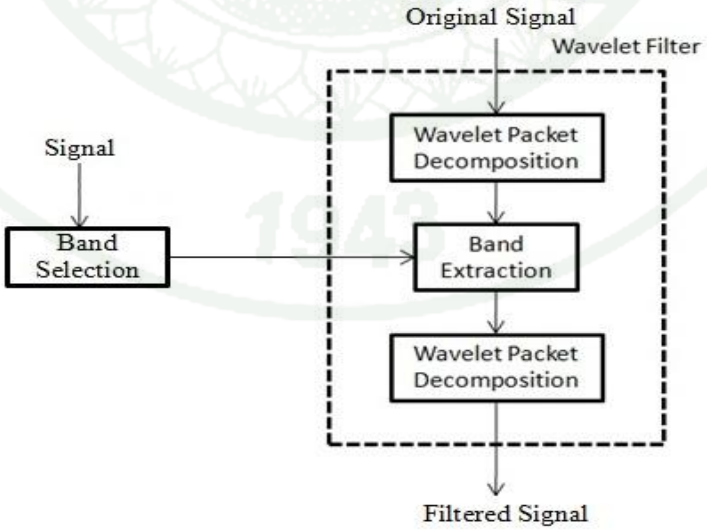

Figure 23 The proposed method of the designed filter.

MATERIALS AND METHODS

Materials

Data Description

BCI competition 2008 data set (Brunner *et al.*, 2008) consists of EEG data from 9 subjects. The cue-based BCI paradigm consisted of four different motor imagery tasks, namely the imagination of movement of the left hand (class 1), right hand (class 2), both feet (class 3), and tongue (class 4). Two sessions on different days were recorded for each subject. Each session is comprised of 6 runs separated by short breaks. One run consists of 48 trials (12 for each of the four possible classes), yielding a total of 288 trials per session. At the beginning of each session, a recording of approximately 5 minutes was performed to estimate the EOG influence. The recording was divided into 3 blocks: (1) two minutes with eyes open (looking at a fixation cross on the screen), (2) one minute with eyes closed, and (3) one minute with eye movements. The timing scheme of one session is illustrated in Figure 24. Note that due to technical problems the EOG block is shorter for subject A04T and contains only the eye movement condition.

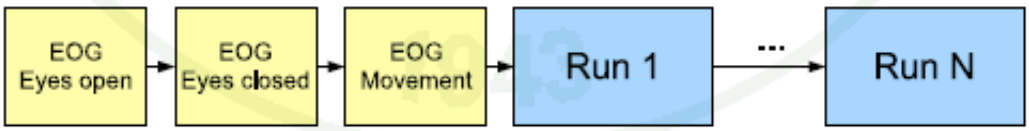

Figure 24 Timing scheme of one session.

Source: Brunner *et al.*, (2008).

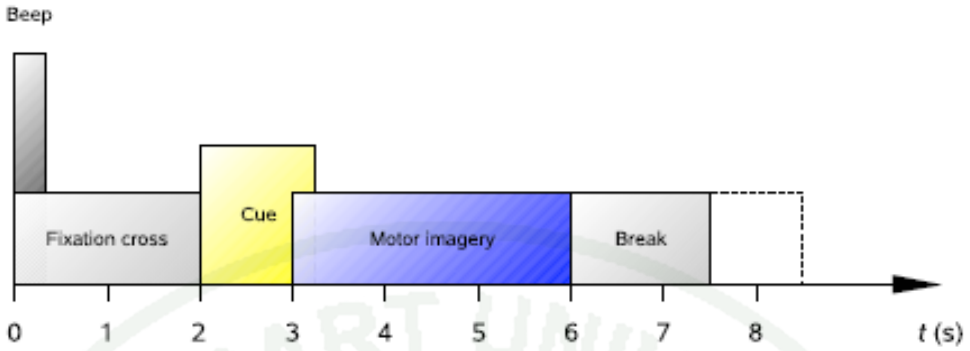

Figure 25 Timing scheme of the paradigm.

Source: Brunner *et al.*, (2008).

The subjects were sitting in a comfortable armchair in front of a computer screen. At the beginning of a trial (t = 0 s), a fixation cross appeared on the black screen. In addition, a short acoustic warning tone was presented. After two seconds (t = 2 s), a cue in the form of an arrow pointing either to the left, right, down or up (corresponding to one of the four classes left hand, right hand, foot or tongue) appeared and stayed on the screen for 1.25 s. This prompted the subjects to perform the desired motor imagery task. No feedback was provided. The subjects were ask to carry out the motor imagery task until the fixation cross disappeared from the screen at t = 6 s. A short break followed where the screen was black again. The paradigm is illustrated in Figure 25. Twenty-two Ag/AgCl electrodes (with inter-electrode distances of 3.5 cm) were used to record the EEG; the montage is shown in Figure 26 left. All signals were recorded monopolarly with the left mastoid serving as reference and the right mastoid as ground. The signals were sampled with 250 Hz and bandpass-filtered between 0.5 Hz and 100 Hz. The sensitivity of the amplifier was set to 100 μV. An additional 50 Hz notch filter was enabled to suppress line noise.

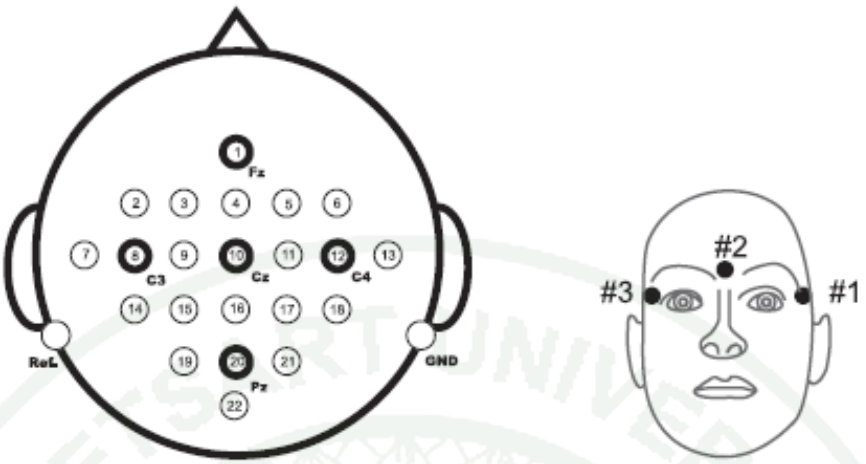

Figure 26 Left: Electrode montage corresponding to the international 10-20 system. Right: Electrode montage of the three monopolar EOG channels.

Source: Brunner *et al.*, (2008).

Methods

1. Data Rereferencing

A study of a suitable EEG reference is important because the reference will influence in the BCIs. In BCI competition 2008, the data set were recorded monopolarly with the left mastoid as reference and right mastoid as ground. Monopolar recording may cause a contaminated problem. Therefore, we need to study EEG rereferencing. This thesis will test Monopolar, Bipolar, Laplacian, and Common Average Referenced (CAR).

Researchers use one differential amplifier per a pair of electrodes. A differential amplifier gains voltage between the active electrode and the reference normally, 1,000-100,000 times. In monopolar recording, the electrode at left mastoid is connected to input 2 of all amplifiers as reference, and the active electrodes are connected to input 1 of each amplifier. In bipolar recording, an anterior electrode is connected to input 1 of each amplifier, and a posterior electrode is connected to the other input. Laplacian recording is implemented by subtracting averaged four neighborhood channels from the channel of interest. CAR recording is similar to monopolar recording, but reference of CAR is mean of all electrodes instead.

2. Frequency Filtering

EEG signal in motor imagery must be filtered in an 8-30 Hz band involving with a motor activity (MU and Beta bands). We use Finite Impulse Response (FIR) Filter to implement 8-30 Hz bandpass filters. The FIR filters with odd symmetric coefficients shown in Figure 27 result in linear phase response, which is a crucial characteristic in signal processing. The FIR filters can be designed by the window method. This thesis will test filters designed by the window method namely Rectangular, Hanning, Bartless, Hamming, Blackman, and Kaiser windows. Figure 28 shows the shape of the windows and their impulse responses.

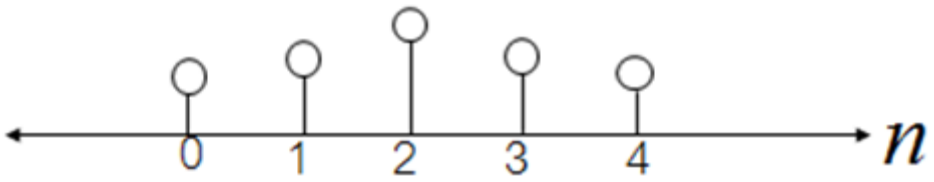

Figure 27 Odd symmetric impulse response.

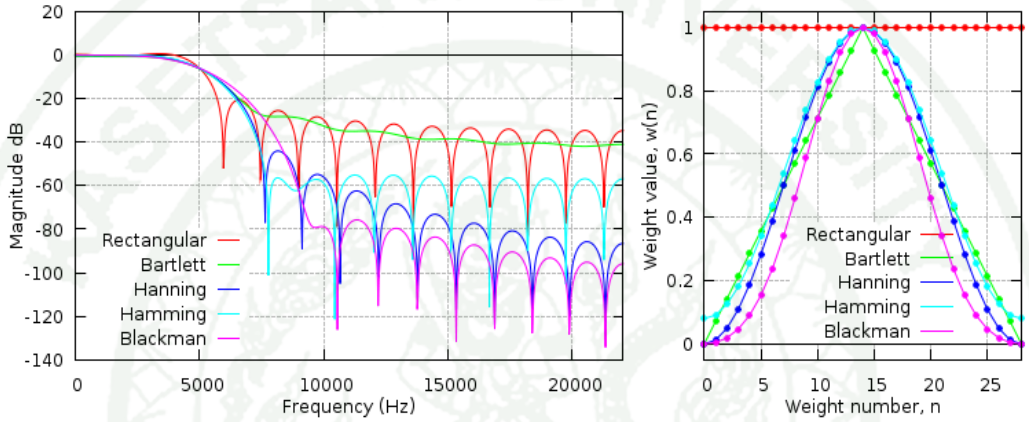

Figure 28 Left: Characteristics of window designation. Right: Impulse response of each window.

3. Wavelet Packet Transform (WPT)

As informative patterns occur from task stimulation, time response of each brain is not equal. A variety of pattern occurrence results in non-stationary signal. In motor imagery, the pattern is located in 8-30 Hz range which covers MU and Beta bands. Because of non-stationary signal, signal analysis must concern not only with frequency domain but with time domain also. Therefore, Short Time Fourier Transform (STFT), which is one of the most useful time-frequency transforms, is used for analyzing non-stationary signal. Wavelet Transform (WT) (Selesnick, 2007) was developed as an alternative analysis to overcome the fixed window problem in STFT. Mother wavelets, similar to window in STFT, can adjust their shapes by shifts and dilation parameters. Discrete Wavelet Transform (DWT) can be implemented by half cut-off high-pass and low-pass filters. The output of the high-pass filter is represented

as details, and the output of the low-pass filter is represented as approximation. The approximation will be decomposed into detail and approximation in the next level further. However, details that are not computed in lower levels may contain significant information. Consequently, WPT will compute details as well to remain information and provide more frequency resolutions.

4. Band Selection

In band selection, we intend to select the most informative frequency bands for each individual. The bands are selected by a discriminative value. The value can be determined by energy of wavelet coefficients seeing more details Appendix A. The pre-processed signal is decomposed by the decomposition. However, because the packet decomposition produces 2^{level} subbands, it's redundant. Therefore, we should reduce dimensions of the decomposition by finding an optimal tree (the best-basis paradigm).

Local Discriminant Bases (LDB) algorithm (Saito and Coifman, 1995) has been used in the dimensional reduction. LDB will find an optimal tree following a discriminative value with the bottom-up search. As an objective of this algorithm is to select an efficient tree, there is no any information loss after this process. The bands in the tree are sorted by the discriminative value. Because high discriminative values mean highly different patterns between the two classes, we will select the highest-valued band(s) in order to implement in the further adaptive filter.

5. Wavelet Filter

Owning to the perfect reconstruction property of the wavelet transform, it's able to implement a band-pass filter. The filter is computed by decomposing and reconstructing only the selected bands. First, original signal is decomposed by WPD, and then we select bands from the previous process and remove other bands by setting all values in the undesirable subbands to zeros. Subsequently, the reconstructed signal is the band-pass filtered signal (XiaoNan *et al.*, 2010).

6. Feature Extraction

The characteristic finding to represent the signal is called Feature Extraction. The feature is directly related to classification accuracy because if we choose good features representing the signal, the feature will contain information enough to be identified. In this thesis, we consider variances of CSP signal as features that popularly represent EEG signal. It's well known that raw EEG signal has a poor spatial resolution because of volume conduction. Thus, the signal of interest can only be observed after appropriate signal processing. The most useful approach is Common Spatial Pattern (CSP) technique (Ramoser *et al.*, 2000). This approach calibrates the system specific for each user. Besides, CSP technique maximizes variance of the filtered signal under one condition (classify left and right hand motor imagery), while minimizing it for other conditions. In CSP analysis, EEG data are represented as an $N \times T$ matrix E, where N is a number of channels and T is a number of task samples. First, the normalized covariance is obtained by Equation 1, where the *trace* function is summation of the diagonal matrix.

$$C = \frac{EE'}{trace(EE')} \tag{1}$$

In this paper, we will classify between left hand (l) and right hand (r) motor imagery tasks. Thus, $\bar{C}_l$ is calculated by averaging over the trials of the left hand task group, and $\bar{C}_r$ is calculated similarly. $\bar{C}_c$, which is the spatial covariance, can find eigenvalues and eigenvectors following Equation 2-3. U_c is the matrix of the eigenvectors and λ_c is the diagonal matrix of the eigenvalues. Before next processing, the eigenvectors in matrix U_c are sorted in descending order of the eigenvalues in matrix λ_c.

$$\bar{C}_C = \bar{C}_l + \bar{C}_r \tag{2}$$

$$\bar{C}_C = U_C \lambda_C U_C' \tag{3}$$

To decorrelate relationship among variables, the whitening transformation has been used.

$$P = \sqrt{\lambda_C^{-1} U_C'} \tag{4}$$

Subsequently, during decorrelation in Equation 5-6, $\overline{C}_l$ and $\overline{C}_r$ are transformed to $\overline{S}_l$ and $\overline{S}_r$ by using matrix P in Equation 4 resulting in the shared eigenvector matrix. Equation 7 shows the shared eigenvalues of each class, where I is the identity matrix. λ_l and λ_r are the eigenvalue matrix of each class after the whitening transforming, and B is the transformed eigenvector matrix. Therefore, the eigenvector with the largest eigenvalue in $\overline{S}_l$ has the smallest eigenvalue in $\overline{S}_r$.

$$\overline{S}_l = P\overline{C}_l P' \,,\ \overline{S}_r = P\overline{C}_r P' \tag{5}$$

$$\overline{S}_l = B\lambda_l B' \,,\ \overline{S}_r = B\lambda_r B' \tag{6}$$

$$\lambda_l + \lambda_r = I \tag{7}$$

To construct the projection matrix as Equation 8, first and last m eigenvector of matrix B are chosen, where W is the transformation that uses for the later data.

$$W = B'P \tag{8}$$

$$Z = WE \tag{9}$$

When the signal matrix E multiplies the transformation W, Z is the CSP signal matrix following Equation 9. Because the transformation maximizes variance of the signal, features representing the signal should be the variance computed from Equation 10, where p is a number of channels of interest. Function *var* is variance of the signal.

$$f_p = \log\left(\frac{\text{var}(Z_p)}{\sum_{i=1}^{2m}\text{var}(Z_i)}\right) \quad (10)$$

7. Classifier

A learning machine that is able to recognize patterns of a signal must be trained by these features of the pattern. Most learning machine techniques are used in pattern recognition as classifiers. Several classifiers are available, but Bayes Classifier based on probability is chosen in this thesis. Bayes decision models Guassian equations from mean and variance of the two-class training set in order to recognize the patterns. Bayes Decision Theory has been proposed as a classifier which is about to probabilistic terms terms (Kolmorgen and Blanertz, 2002). The solution of Bayes theory is to maximize the posterior probabilities $P(\omega_i \mid x)$. However, $P(\omega_i \mid x)$ cannot be directly calculated, but Bayes formula allows us to calculate $P(\omega_i \mid x)$ from the prior probabilities $P(x \mid \omega_i)$ and the probability of each class $P(\omega_i)$ given as equation 11. The feature probability $P(x)$ can be ignored because it must be equal every comparison. Features that represent the signal each class are calculated the posterior probability by equation 12.

$$P(\omega_i \mid x) = \frac{P(x \mid \omega_i)P(\omega_i)}{P(x)} \quad (11)$$

If the features belonging to which class have the probability higher than that of the other one, the signal represented by these features will be decided as this class.

$$g_i(x) = \ln P(x \mid \omega_i) + \ln P(\omega_i) \quad (12)$$

$$g(x) = g_1(x) - g_2(x) \quad (13)$$

As a result, one of the most convenient ways to classify patterns is to use the decision function in Equation 13. The decision rule is able to classify a two-class data by deciding as class 1 when $g(x) > 0$; otherwise deciding as class 2.

8. Procedure

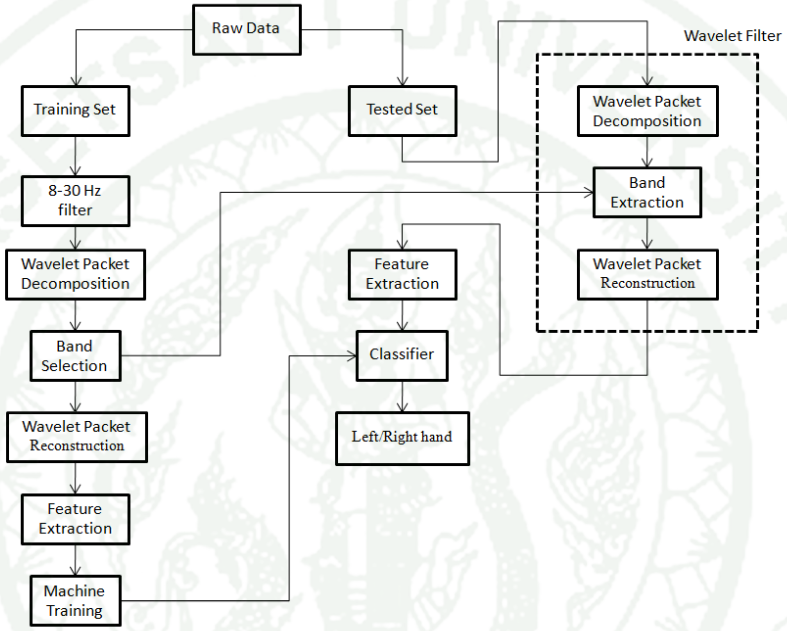

Figure 29 Flow chart of the experiment.

To follow the flow chart in Figure 29, the data set is equally separated into 2 sets: training set and tested set. The training set is filtered by Kaiser 8-30 Hz band-pass filter to remove irrelevant frequency components. Next, the filtered signal is decomposed into binary-tree subbands, and the subbands are sorted by the discriminative value. The highest-valued bands are selected as appropriate bands in order to use in the adaptive filter designation. The adaptive filter is used for both training set and tested set. After adaptive filtering, the filtered signal is extracted features. The learning machine is trained by these features by Bayes decision theory. The theory models probabilistic equations to classify the patterns. For the tested set, it is filtered by the wavelet filter. Then, the filtered signal is extracted the features. Finally, Bayes equation is applied to classify the test set.

RESULTS AND DISCUSSION

Results

First of all, we trim the data set into trials. Each the EEG signal is cut from t=3s to t=6s of each execution, and the signal is sampled at 250 Hz. Therefore, the signal has 750 samples. Average of all trials (channel C_3 and C_4) are shown in Figure 30. The next step is to filter the signal in order to remove irrelevant frequency components. The FIR filter is designed by Kaiser window method. The specification of the designed filter is shown in Figure 31. The signal is filtered by the designed filter, and comparison between the original signal and the filtered signal is shown in Figure 32.

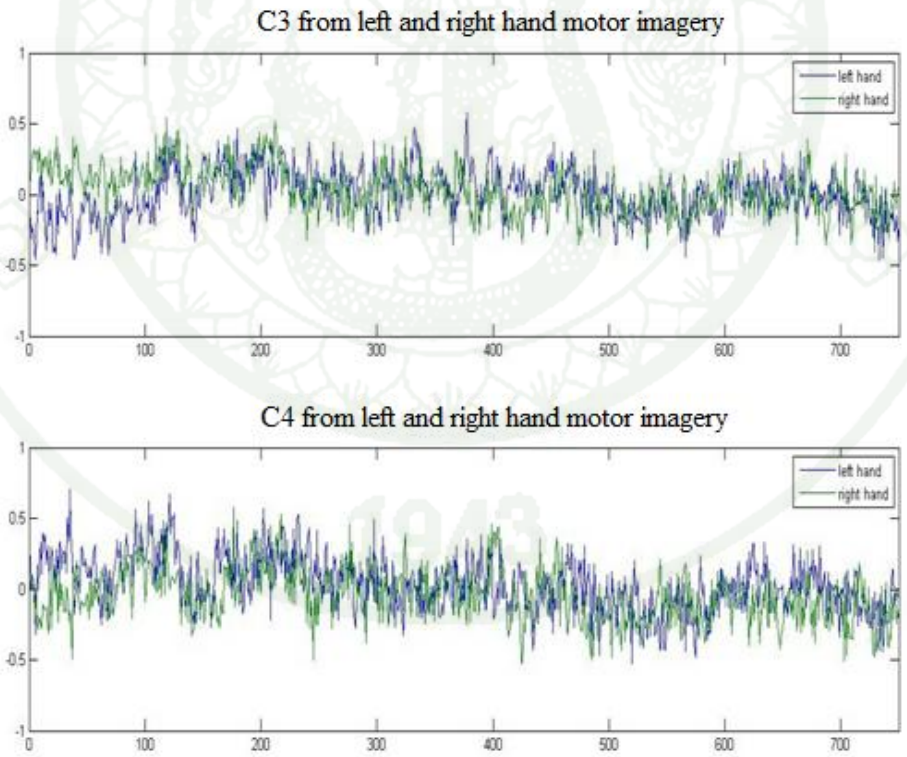

Figure 30 Averaged signal of all trials.

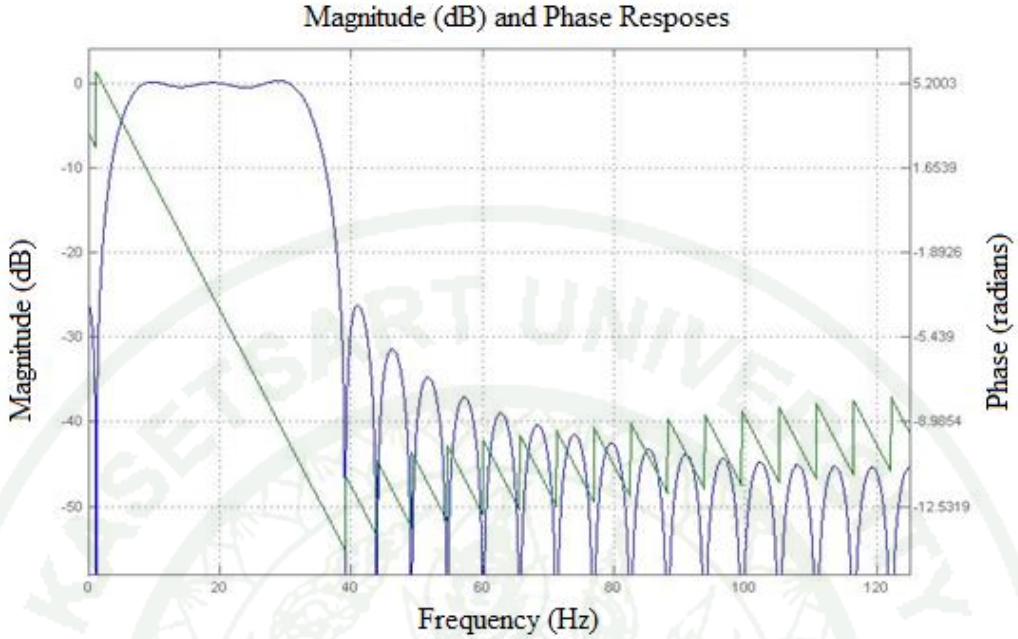

Figure 31 Specification of the designed FIR filter.

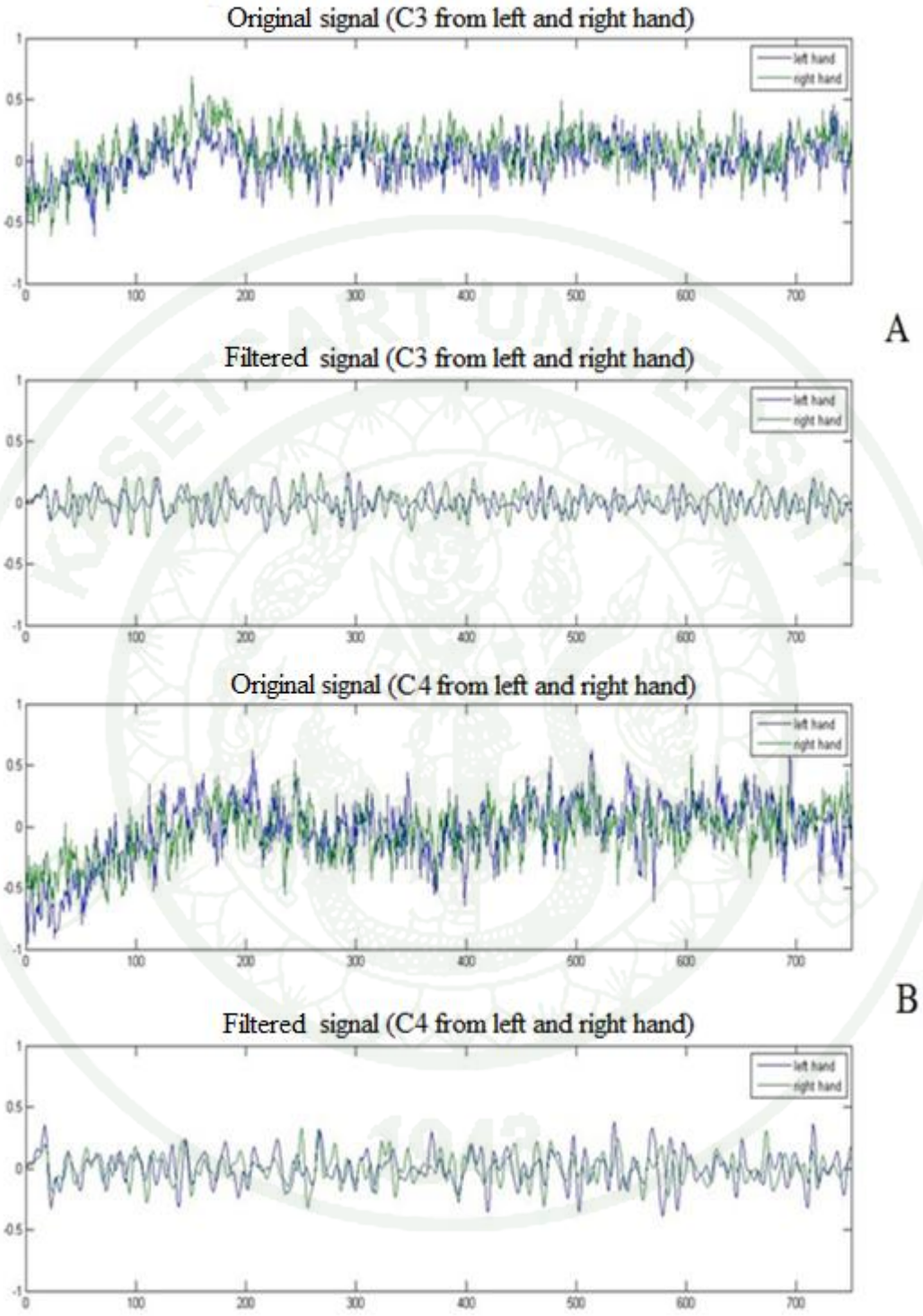

Figure 32 A: Comparison between original signal and filtered signal (channel C_3). B: Comparison between original signal and filtered signal for (channel C_4).

In the band selection, the signal needs decomposing by WPD. The signal is decomposed into 6 levels of the packet tree by Daubechies4 mother wavelet shown in Figure 33. The 2^{level} subbands of the tree can be reduced the dimensions by finding an optimum tree using LDB. The bands in the tree are sorted by the discriminative value. We select the highest-valued bands as appropriate bands of each person. For example, in subject A01, the selected band of C_3 and C_4 approximately are 10-12 Hz and 12-16 Hz respectively shown in Figure 34. Next, the wavelet filtered signal is shown in Figure 35.

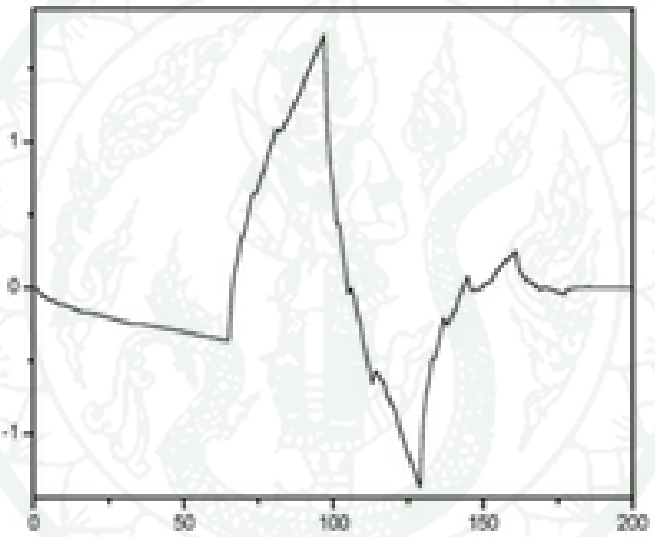

Figure 33 Daubichies4 mother wavelet that uses in the decomposition.

	Band Range (Hz)				
		9.7-11.7	11.7-15.6		
C_3					
C_4					

Figure 34 The best bands produced by subject A01.

After wavelet filtering, the filtered signal is extracted features by CSP technique. The algorithm maximized variance of the filtered signal. Maximization of the filtered signal is shown in Figure 36. Subsequently, we calculate the variance from the processed signal as features. These features are used to train the learning machine. Bayes equations are modeled by the mean and the standard deviation of the features for deciding patterns.

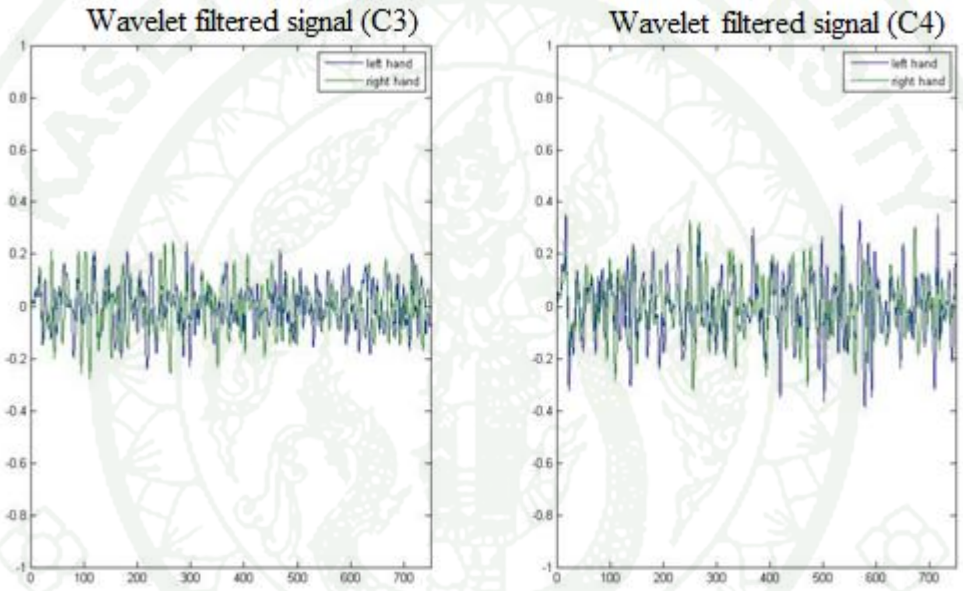

Figure 35 Filtered signal by the wavelet filter.

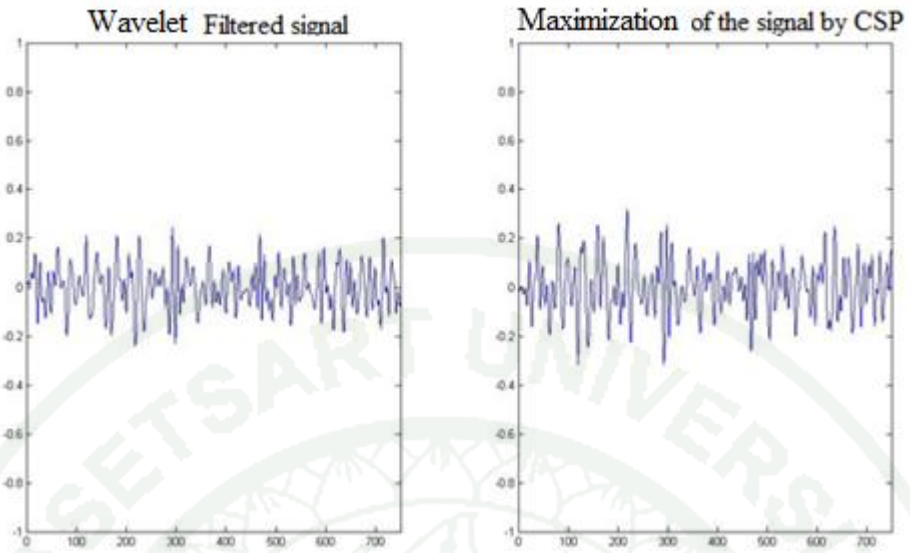

Figure 36 Maximization of the signal by CSP.

1. Rereferencing

Besides, although there are 72 samples per class in training set and test set, some samples for each person are improper to use in classification, which are labeled by experts. Thus, samples of each person may not be equal. The number of samples in the classification is shown in Table1.

Table 1 The number of training and test set.

Person	Task			
	Left training	Left test	Right training	Right test
A01	69	72	69	70
A02	67	71	69	71
A04	62	59	67	57
A05	63	70	66	65
A07	67	71	66	69
A09	53	65	63	65

This thesis studies a reference impact on classification accuracy. Therefore, we vary types of reference in the experiments called rereferencing. After rereferenecing, the EEG signal is filtered and is extracted features by using variances of CSP signal. The features train Bayes classifier for deciding pattern in test set. Then, we select the reference suitable for hand motor imagery task.

Table 2 Classification accuracy of various references (Left hand task).

Reference	Person						
	A01	A02	A04	A05	A07	A09	Average
Mon1	26.76%	64.78%	55.93%	94.28%	26.76%	33.84%	50.39%
Mon2	40.84%	66.19%	88.13%	67.14%	26.76%	76.92%	60.99%
Mon3	57.74%	60.56%	72.88%	90%	61.97%	60%	67.19%
Lap1	90.14%	61.97%	16.94%	55.71%	59.15%	18.46%	50.39%
Lap2	92.95%	80.28%	27.11%	77.14%	59.15%	3.07%	56.61%
Lap3	61.97%	70.42%	81.35%	82.85%	53.52%	78.46%	71.42%
Bi1	70.42%	66.19%	66.10%	87.14%	32.39%	50.76%	62.16%
Bi2	71.83%	94.36%	93.22%	68.57%	85.91%	72.30%	81.03%
CAR1	84.50%	85.91%	27.11%	91.42%	12.67%	23.07%	54.11%
CAR2	81.69%	81.69%	20.33%	72.85%	12.67%	32.30%	50.25%
CAR3	52.11%	85.91%	67.79%	91.42%	70.42%	95.38%	77.17%

Table 3 Classification accuracy of various references (Right hand task).

Reference	Person						
	A01	A02	A04	A05	A07	A09	Average
Mon1	81.42%	28.16%	56.14%	0%	81.15%	76.92%	53.96%
Mon2	91.42%	33.80%	36.84%	26.15%	63.76%	60%	51.99%
Mon3	88.57%	52.11%	38.59%	9.23%	40.57%	72.30%	50.22%
Lap1	40%	47.88%	92.98%	55.38%	95.65%	89.23%	70.18%
Lap2	32.85%	32.39%	73.68%	13.84%	94.20%	100%	57.82%
Lap3	85.71%	45.07%	21.05%	13.84%	53.62%	73.84%	48.85%
Bi1	90%	40.84%	71.92%	1.53%	66.66%	63.07%	55.67%
Bi2	91.42%	5.63%	17.54%	15.38%	17.39%	33.84%	30.20%
CAR1	30%	12.67%	73.68%	12.30%	44.92%	78.46%	42.00%
CAR2	31.42%	22.53%	66.66%	21.53%	62.31%	76.92%	46.89%
CAR3	95.71%	26.76%	40.35%	12.30%	23.18%	21.53%	36.63%

Table 4 Classification accuracy of various references (Both hand task).

Reference	Person						
	A01	A02	A04	A05	A07	A09	Average
Mon1	54.09%	46.47%	56.03%	47.14%	53.96%	55.38%	52.17%
Mon2	66.13%	50%	62.48%	46.64%	45.26%	68.46%	56.49%
Mon3	73.15%	56.33%	55.73%	49.61%	51.27%	66.15%	58.70%
Lap1	65.07%	54.92%	54.96%	55.54%	77.40%	53.84%	**60.22%**
Lap2	62.90%	56.33%	50.41%	45.49%	76.67%	51.53%	57.22%
Lap3	73.84%	57.74%	51.20%	48.35%	53.57%	76.15%	60.14%
Bi1	80.21%	53.52%	69.01%	44.34%	49.53%	56.92%	58.92%
Bi2	81.62%	50%	55.38%	41.93%	51.65%	53.07%	55.60%
CAR1	57.25%	49.29%	50.40%	51.86%	28.80%	50.76%	48.06%
CAR2	56.55%	52.11%	43.50%	47.19%	37.49%	54.61%	48.54%
CAR3	73.91%	56.33%	54.07%	51.86%	46.80%	58.46%	56.90%

Mon1 = two-channel monopolar reference (C_3 and C_4)

Mon2 = three-channel monopolar reference (C_3, C_z, and C_4)

Mon3 = seventeen-channel monopolar reference (C_5, FC_3, C_3, CP_3, FC_1, C_1, CP_1, FC_z, C_z, CP_z FC_2, C_2, CP_2, FC_4, C_4 CP_4, and C_6)

Lap1 = two-channel laplacian reference (C_3 and C_4)

Lap2 = three-channel laplacian reference (C_3, C_z, and C_4)

Lap3 = seventeen-channel laplacian reference (C_5, FC_3, C_3, CP_3, FC_1, C_1, CP_1, FC_z, C_z, CP_z FC_2, C_2, CP_2, FC_4, C_4 CP_4, and C_6)

Bi1 = two-channel bipolar reference (FC_3- CP_3 and FC_4- CP_4)

Bi2 = three-channel bipolar reference (FC_3- CP_3, FC_z- CP_z, and FC_4- CP_4)

CAR1 = two-channel CAR reference (C_3 and C_4)

CAR2 = three-channel CAR reference (C_3, C_z, and C_4)

CAR3 = seventeen-channel CAR reference (C_5, FC_3, C_3, CP_3, FC_1, C_1, CP_1, FC_z, C_z, CP_z FC_2, C_2, CP_2, FC_4, C_4 CP_4, and C_6)

The results in Table 2-4 indicate that “Lap1” is the best result for hand motor imagery. As a result, we used this reference in all our experiments further.

2. Filtering

We then test the various impacts of FIR static filters. The results in Table 5-7 indicate that the Kaiser filter produces the best result.

Table 5 Classification accuracy of various FIR filters (Left hand task).

Filters	Person						
	A01	A02	A04	A05	A07	A09	AVG
Bartlett	87.32%	74.64%	30.50%	55.71%	52.11%	20%	70.18%
Blackman	87.32%	81.69%	57.62%	64.28%	52.11%	24.61%	61.27%
Gaussian	87.32%	74.64%	22.03%	61.42%	49.29%	20%	52.45%
Hamming	87.32%	78.87%	38.98%	64.28%	47.88%	24.61%	56.99%
Hanning	87.32%	78.87%	40.67%	65.71%	47.88%	24.61%	57.51%
Kaiser	90.14%	61.97%	16.94%	55.71%	59.15%	18.46%	50.39%
Rectangular	88.73%	74.64%	22.03%	58.57%	63.38%	20%	54.55%

Table 6 Classification accuracy of various FIR filters (Right hand task).

Filters	Person						
	A01	A02	A04	A05	A07	A09	AVG
Bartlett	50%	32.39%	61.40%	47.69%	62.31%	90.76%	57.42%
Blackman	47.14%	29.57%	42.10%	44.61%	60.86%	90.76%	52.50%
Gaussian	54.28%	30.98%	87.71%	46.15%	78.26%	93.84%	65.20%
Hamming	52.85%	30.98%	50.87%	43.07%	60.86%	90.76%	54.89%
Hanning	52.85%	30.98%	42.10%	41.53%	60.86%	90.76%	53.18%
Kaiser	40%	47.88%	92.98%	55.38%	95.65%	89.23%	70.18%
Rectangular	52.85%	33.80%	87.71%	49.23%	75.36%	93.84%	65.46%

Table 7 Classification accuracy of various FIR filters (Both hand task).

Filters	Person						
	A01	A02	A04	A05	A07	A09	AVG
Bartlett	68.66%	53.52%	45.95%	51.70%	57.21%	56.15%	55.53%
Blackman	67.23%	55.63%	49.86%	54.45%	56.49%	57.69%	56.89%
Gaussian	70.80%	52.81%	54.87%	53.79%	63.77%	56.92%	58.82%
Hamming	70.09%	54.92%	44.93%	53.68%	54.37%	57.69%	55.94%
Hanning	70.09%	54.92%	41.39%	53.62%	54.37%	57.69%	55.34%
Kaiser	65.07%	54.92%	54.96%	55.54%	77.04%	53.84%	**60.22%**
Rectangular	70.79%	54.22%	54.87%	53.90%	69.37%	56.92%	60.01%

As a consequence, we will use the two-channel Laplacian reference with Kaiser window filtering as a benchmark.

3. Individual Results

3.1 Subject A01

For person 1, "A01", we make this experiment to test our proposed filter by varying the number of remaining bands. While Kaiser filtering produces the best result in static filters, the adaptive filter using the highest-valued band can improve the result of the pervious method from 65.07 % to 68.16 %. Classification accuracy of the improvement is shown in Table 8.

Table 8 Classification accuracy of the proposed method (A01).

The number of band reconstruction	Accuracy (%)		
	Left	Right	All
10	99.29	12.85	55.72
9	100	2.85	51.42
8	100	4.28	52.14
7	100	2.85	51.42
6	100	2.85	51.42
5	100	2.85	51.42
4	100	2.85	51.42
3	100	0	50
2	100	0	50
1	**56.33**	**80**	**68.16**
The Kaiser filter (8-30 Hz)	90.14	40	65.07

Table 9 shows the remaining band of C_3 and C_4. The number of remaining bands of C_3 and C_4 must be equal. In this person, the appropriate band of C_3 is S(6,5) equivalent 9.76-11.71 Hz, and the appropriate band of C_4 is S(5,3) equivalent 11.71-15.62 Hz.

Table 9 The remaining band of C_3 and C_4 (A01).

The remaining band for C_3	Frequency range (Hz)
S(6,5)	9.76-11.71

The remaining band for C_4	Frequency range (Hz)
S(5,3)	11.71-15.62

4.2 Subject A02

For person 2, “A02”, we make this experiment to test our proposed filter by varying the number of remaining bands. While Kaiser filtering produces the best result in static filters, the adaptive filter using the highest-valued bands can improve the result of the pervious method from 54.92 % to 61.97 %. Classification accuracy of the improvement is shown in Table 10.

Table 10 Classification accuracy of the proposed method (A02).

The number of band reconstruction	Accuracy (%)		
	Left	Right	All
10	83.09	33.80	58.45
9	90.14	25.35	57.74
8	76.05	45.07	60.56
7	88.73	33.80	61.26
6	92.95	22.53	57.74
5	83.09	40.84	61.97
4	**83.09**	**40.84**	**61.97**
3	80.28	36.61	58.45
2	84.50	15.49	50
1	83.09	22.53	52.81
The Kaiser filter (8-30 Hz)	61.97	47.88	54.92%

Table 11 shows the remaining bands of C_3 and C_4. In this person, the appropriate band of C_3 is S(6,12), S(6,6), S(6,0), and S(5,2) equivalent 23.43-25.39 Hz, 11.71-13.67 Hz, 0-1.95 Hz, and 7.8-11.71 Hz. The appropriate band of C_4 is S(4,1), S(6,12), S(6,0), and S(6,14) equivalent 7.81-15.62 Hz, 23.43-25.39 Hz, 0-1.95 Hz, and 27.34-29.29 Hz.

Table 11 The remaining bands of C_3 and C_4 (A02).

The remaining bands for C_3	Frequency range (Hz)
S(6,12)	23.43-25.39
S(6,6)	11.71-13.67
S(6,0)	0-1.95
S(5,2)	7.8-11.71

The remaining bands for C_4	Frequency range (Hz)
S(4,1)	7.81-15.62
S(6,12)	23.43-25.39
S(6,0)	0-1.95
S(6,14)	27.34-29.29

4.3 Subject A04

For person 3, “A04”, we make this experiment to test our proposed filter by varying the number of remaining bands. While Kaiser filtering produces the best result in static filters, the adaptive filter using the highest-valued bands can improve the result of the pervious method from 54.96 % to 60.83 %. Classification accuracy of the improvement is shown in Table 12.

Table 12 Classification accuracy of the proposed method (A04).

The number of band reconstruction	Accuracy (%)		
	Left	Right	All
10	27.11	85.96	56.54
9	27.11	89.47	58.29
8	23.72	82.45	53.09
7	3.38	85.96	44.67
6	3.38	85.96	44.67
5	18.64	80.70	49.67
4	22.03	73.68	47.85
3	18.64	89.47	54.05
2	**32.20**	**89.47**	**60.83**
1	20.33	89.47	54.90
The Kaiser filter (8-30 Hz)	16.94	92.98	54.96

Table 13 shows the remaining bands of C_3 and C_4. In this person, the appropriate band of C_3 is S(5,7) and S(6,12) equivalent 27.34-31.25 Hz and 23.43-25.39 Hz. The appropriate band of C_4 is S(6,5) and S(4,3) equivalent 9.76-11.71 Hz and 23.43-31.25 Hz.

Table 13 The remaining bands of C_3 and C_4 (A04).

The remaining bands for C_3	Frequency range (Hz)
S(5,7)	27.34-31.25
S(6,12)	23.43-25.39

The remaining bands for C_4	Frequency range (Hz)
S(6,5)	9.76-11.71
S(4,3)	23.43-31.25

4.4 Subject A05

For person 4, “A05”, we make this experiment to test our proposed filter by varying the number of remaining bands. While Kaiser filtering produces the best result in static filters, the adaptive filter using the highest-valued bands can improve the result of the pervious method from 55.54 % to 58.35 %. Classification accuracy of the improvement is shown in Table 14.

Table 14 Classification accuracy of the proposed method (A05).

The number of band reconstruction	Accuracy (%)		
	Left	Right	All
10	17.41	86.15	51.64
9	15.71	86.15	50.93
8	15.71	84.61	50.16
7	18.57	78.46	48.51
6	97.14	3.07	50.10
5	87.14	18.46	52.80
4	64.28	49.23	56.75
3	**62.85**	**53.84**	**58.35**
2	100	9.23	54.61
1	67.14	27.69	47.41
The Kaiser filter (8-30 Hz)	55.71	55.38	55.54

Table 15 shows the remaining bands of C_3 and C_4. In this person, the appropriate band of C_3 is S(6,6), S(6,7), and S(6,0) equivalent 11.71-13.67 Hz, 13.67-15.62 Hz, and 0-1.95 Hz. The appropriate band of C_4 is S(6,6), S(6,2), and S(6,7) equivalent 11.71-13.67 Hz, 3.9-5.85 Hz, and 13.67-15.62 Hz.

Table 15 The remaining bands of C_3 and C_4 (A05).

The remaining bands for C_3	Frequency range (Hz)
S(6,6)	11.71-13.67
S(6,7)	13.67-15.62
S(6,0)	0-1.95

The remaining bands for C_4	Frequency range (Hz)
S(6,6)	11.71-13.67
S(6,2)	3.9-5.85
S(6,7)	13.67-15.62

4.5 Subject A07

For person 5, “A07”, we make this experiment to test our proposed filter by varying the number of remaining bands. This is a case that Kaiser filtering produces the best result, whereas the adaptive filter using the highest-valued band(s) cannot improve the result of the pervious method shown in Table 16.

Table 16 Classification accuracy of the proposed method (A07).

The number of band reconstruction	Accuracy (%)		
	Left	Right	All
10	43.66	88.40	66.03
9	42.25	88.40	65.32
8	**67.60**	**75.36**	**71.48**
7	63.38	76.81	70.09
6	60.56	73.91	67.23
5	78.87	40.57	59.72
4	66.19	17.39	41.79
3	50.70	23.18	36.94
2	97.18	4.34	50.76
1	57.74	39.13	48.43
The Kaiser filter (8-30 Hz)	59.15	95.65	77.40

4.6 Subject A09

For person 6, “A09”, we make this experiment to test our proposed filter by varying the number of remaining bands. While Kaiser filtering produces the best result in static filters, the adaptive filter using the highest-valued band can improve the result of the pervious method from 53.84 % to 62.30 %. Classification accuracy of the improvement is shown in Table 17.

Table 17 Classification accuracy of the proposed method (A09).

The number of band reconstruction	Accuracy (%)		
	Left	Right	All
10	15.38	98.46	56.92
9	20	98.46	59.23
8	20	98.46	59.23
7	16.92	98.46	57.69
6	15.38	98.46	56.92
5	15.38	98.46	56.92
4	15.38	98.46	56.92
3	20	98.46	59.23
2	16.92	98.46	57.69
1	**26.15**	**98.46**	**62.30**
The Kaiser filter (8-30 Hz)	18.46	89.23	53.84

Table 18 shows the remaining band of C_3 and C_4. In this person, the appropriate band of C_3 is S(6,7) equivalent 13.67-15.62 Hz. The appropriate band of C_4 is S(6,7) equivalent 13.67-15.62 Hz.

Table 18 The remaining bands of C_3 and C_4 (A09).

The remaining band for C_3	Frequency range (Hz)
S(6,7)	13.67-15.62

The remaining band for C_4	Frequency range (Hz)
S(6,7)	13.67-15.62

5. Overall results

The proposed method improves the classification accuracy comparing with the benchmark method (the best static filter). Our adaptive filter produce results more accurate than that of Kaiser filter (the benchmark). Comparison between the benchmark and the proposed method is shown in Table 19-21. The improvement of using the proposed method is approximately 3.5 %.

Table 19 The improvement of using the proposed method (Left hand task).

Filters	Person						
	A01	A02	A04	A05	A07	A09	AVG
Kaiser	90.14%	61.97%	16.94%	55.71%	59.15%	18.46%	50.39%
Proposed	56.33%	83.09%	32.20%	62.85%	67.60%	26.15%	54.70%

Table 20 The improvement of using the proposed method (Right hand task).

Filters	Person						
	A01	A02	A04	A05	A07	A09	AVG
Kaiser	40%	47.88%	92.98%	55.38%	95.65%	89.23%	70.18%
Proposed	80%	40.84%	89.47%	53.84%	75.36%	98.46%	72.99%

Table 21 The improvement of using the proposed method (Both hand task).

Filters	Person						
	A01	A02	A04	A05	A07	A09	AVG
Kaiser	65.07%	54.92%	54.96%	55.54%	77.04%	53.84%	60.22%
Proposed	68.16%	61.97%	60.83%	58.35%	71.48%	62.30%	63.84%

Discussion

BCI competition 2008 provides data set for motor imagery. While they were recording, the experts marked trails that should not use in experiments because of subject mistake or artifacts. Therefore, we need to cut some unusable trails out following the provider suggestion.

In the training process, the raw signal needs to be filtered by an 8-30Hz band-pass filter because the signal must be sure that it will contain only activities related to hand motor imagery. On the other hand, the test process doesn't need the filter as the adaptive filter which is trained by the proposed method should select appropriate bands already.

Before selecting the bands the decomposed tree should be reduced dimensions. We use Local Discriminant Bases (LDB) to find the optimum tree. Now, we have reduced dimensions from 2^{level} subbands to appropriate bands, but there is no loss after this process. In the reduction and selection the appropriate band, it also uses a discriminative value. The values can be found by several functions, but in this experiment, we use energy of wavelet coefficients using Daubichies4 mother wavelet.

The classification uses Bayes classifier related to probabilities. Because the classifier has no a random function, results of the classification every training must be the same.

CONCLUSION AND RECOMMENDATIONS

Conclusion

In hand motor imagery, the two-channel (C_3 and C_4) Laplacian reference with Kaiser filtering is selected because the reference produces the best result in the experiment. A main problem of EEG signal is that brain activity of each person has different frequency components. Therefore, significant information of each person lies on different frequency bands. We have to select highly information bands for each person by using an adaptive filter. The proposed adaptive filter implemented by Wavelet Transform is able to select the most informative bands using a discriminative value in order to eliminate undesirable frequency components. The proposed method can improve classification accuracy from the benchmark. In summary, every BCI system should be designed for each person because the specific system can produce the best result. If the BCI system can better communicate between a brain and computers, we will utilize abundant benefices from the system.

Recommendations

Each subject has not only different informative bands but also various activated areas. For this reasons, we have to design a system specific for each user. In this thesis, we design the adaptive filter based on band selection using the discriminative value. The value plays an important role in measuring difference of patterns. For the first aspect, the further research should study about cost functions which are the most appropriate for hand motor imagery.

In addition, the second aspect is that positions of electrodes producing informative patterns represent by a pair of electrodes (C_3 and C_4 for this thesis). The subsequent research should find out the best pair of electrodes for each person in motor imagery tasks.

LITERATURE CITED

Anderson, C. W. and Sijercic, Z. 1996. Classication of EEG signals from four subjects during five mental tasks. **Proceeding of the International Conference on Engineering Application of Neural Networks**. Available Source: http://www.bbci.de/competition/iv/desc_2a.pdf.

Bao GuoXu and Ai Guo Song. 2008. Pattern recognition of motor imagery EEG using wavelet transform Pattern recognition of motor imagery EEG using wavelet transform. **J. Biomedical Science and Engineering**(1): 64-67.

Brunner, C., Leeb, R., Müller-Putz, G. R., Schlögl, A., and Pfurtscheller, G. 2008. **BCI Competition 2008 Graz data set A.**

Chen Xiao Nan and Xu Zhiyuan, Suo Jidong. 2010. Bandpass Filter Design Based on Wavelet Packet. College of Information Science and Technology. **Dalian Maritime University**, Dalian, China.

Fay S. Tyner, John R. Knott, and Brem Mayer, W. Jr. 1983. **Fundamentals of EEG Technology Volume 1: Basic Concept and Methods.** Lippincott William & Wilkins, Philadelphia, United States.

Herbert Ramoser, Johannes, Müller-Gerking, and Pfurtscheller, G. 2000. Optimal Spatial Filtering of Single Trial EEG During Imagined Hand Movement. **IEEE Transaction on Rehabilitation Engineering**(8).

Ivan W. Selesnick. 2007. **Wavelet Transform –A Quick Study**. Polytechnic University, Brooklyn, New York.

Jen Kolmorgen and Benjarmin Blanertz. 2002. Bayes Classification of Single-Trial Event-Related Potentials in EEG. **Proceeding of the International Conference on Artificial Neural Networks**.

José del Millá, Pierre W. Pierrez, FerranGalán, Eileen Lew, and Ricardo Chavarriaga. 2007. NON-INVASIVE BRAIN-MACHINE INTERACTION. **International Journal of Pattern Recognition and Artificial Intelligence**: 1-3.

Kai Keng Ang, Zheng Yang Chin, Haihong Zhang, and Cuntai Guan. 2008. Filter bank common spatial pattern (FBCSP) in brain-computer interface. **International Joint Conference on Neural Networks**.

Kaper, M., Meinicke, P., Grossekathoefer, U., Lingner, T., and Ritter, H.. 2004. BCI competition 2003data set iib: support vector machines for the p300 speller paradigm. **IEEE Transactions on Biomedical Engineering**(51): 1073-1076.

Kavitha P. Thomas, Cuntai Guan, Chiew Tong Lau, Vinod, A. P., and Kai Keng Ang. 2009. A new discriminative common spatial pattern method for motor imagery brain-computer interface. **IEEE Transaction on Biomedical**(56).

Martin Vetterli. 1992. Wavelets and Fliter Banks: Theory and Design. **IEEE Transaction on Signal Processing**(40).

Millán, J.R. and Mouriño, J. 2003. Asynchronous BCI and local neural classifiers: An overview of the Adaptive Brain Interface project**. IEEE Transaction on Neural Systems and Rehabilitation Engineering, Special Issue on Brain-Computer Interface Technology**.

Naoki Saito and Ronald R. Coifman. 1995. Local Discriminant Bases and Their Applications. **Journal of Mathematical Imaging and Vision**(5): 337-358.

Pfurtscheller, G. and Lopes da Sila, F.H. 1999. Event-related EEG/MEG synchronization and desynchronization: basic principles. **Clinical Neurophysiology**(110): 1842-1857.

Pfurtscheller, G., Brunner, C., Schlögl, A., and Lopes daSila, F.H. 2006. Mu Rhythm (de)synchronization and EEG signal-trial classification of different motor imagery tasks. **NeuroImage**(31): 153-159.

Pfurtscheller, G., Neuper, C., Flotzinger, D., and Pregenzer, M. 1997. EEG-based discrimination between imagination of right and left hand movement. **Electroencephalography and Clinical Neurophysiology**(103): 642-651.

Pfurtscheller, G., Niedermayer, E., and Lopes Da Silva, F. 1999. EEG event-related desynchronization (ERD) and event-related synchronization (ERS). **Electroencephalography: Basic Principles, Clinical Applications and Related Fields.** Lippincott William & Wilkins, Philadelphia, United States.

Schlögl, A., Lee, F., Bischof, H., and Pfurturtscheller, G. 2005. Characterization of four-class motor imagery EEG data for the BCI-competition 2005**. Journal of Neural Engineering**.

Solhjoo, S., Nasrabadi, A.M., and Golpayegani, M. R. H. 2005. Classification of chaotic signals using HMM classifier: EEG-based mental task classification. **Proceeding of the European Signal Processing Conference**.

Stephan Waldert, Tobias Pistohl, Christoph Braun, Tonio Ball, Ad Aertsen, and Carsten Mehring. 2009. A review on directional information in neural signals for brain-machine interfaces. **Journal of Physiology**(103): 244-254.

Thom F. Oostendorp and Adriaan van Oosterom. 1996. The Surface Laplacian of the Potential: Theory and Application. **IEEE Transactions on Biomadical Engineering**(43).

Wu Ting, Yan Guo-zheng, Yang Bang-hua, and Sun Hong. 2008. EEG feature extraction based on wavelet packet decomposition for brain computer interface. **Measurement**(41): 618–625.

APPENDICES

Appendix A

The cost function (energy of wavelet coefficients)

A function that computes the values is called a cost function. Therefore, the high discriminative value means high difference of patterns between the two classes. We consider the cost function based on WPT and Euclidean Distance following Equation (A-C) [8]. Let's denote $W_{i,j,l}(x_i^{(c)})$ as the decomposition coefficients of signal x_i^c at the subband $S(j,k)$, where l is the index of the location of the decomposition coefficients. Let N_C be the number of signals belonging to class c. $e^c(j,k)$ is the normalized energy vector of class c, D is Euclidean Distance, and $H(S(j,k))$ is the discriminant power of the subband. As a consequence, the highest-valued bands are selected as appropriate bands.

$$H(S(j,k)) = \sum_{c=1}^{C-1} \sum_{m=c+1}^{C} D(e^{(c)}(j,k), e^{(m)}(j,k)) \quad \text{(A)}$$

$$e^{(c)}(j,k) = [e^{(c)}(j,k,0);..;e^{(c)}(j,k,2^{n_0-j}-1)] \quad \text{(B)}$$

$$e^{(c)}(j,k,l) = \frac{\sum_{i=1}^{N_C} (W_{j,k,l}(x_i^c))^2}{\sum_{i=1}^{N_C} \left\| x_i^c \right\|^2} \quad \text{(C)}$$

Appendix B

ICICTES publication

The International Conference on Information and Communication Technology for Embedded Systems

Amari Orchid, Pattaya, Thailand 27-29 January 2011

ICICTES 2011

IMPORTANT DATES

1 Nov. 2010 Paper Submission
1 Dec. 2010 Author Notification
13 Dec. 2010 Camera Ready and Early Registration Deadline

ORGANIZING COMMITTEE

Honorary Chairs:
- Nobuo Fujii, Tokyo Institute of Technology
- Vudtechai Kapilakanchana, President of Kasetsart University
- Surapon Nitikraipot, Rector of Thammasat University
- Pansak Siriruchatapong, Director of NECTEC

General Chairs (Conference Chairs):
- Asanee Kawtrakul, Vice Director, NECTEC
- Hiroaki Kunieda, Tokyo Institute of Technology
- Somnuk Sirisoonthorn, NSTDA
- Nontawat Junjareon, Kasetsart University
- Chongrak Polprasert, SIIT, Thammasat University

Technical Program Chairs:
- Tsuyoshi Isshiki, Tokyo Institute of Technology
- Kanokvate Tungpimolrut, NECTEC
- Pisut Raphisak, Kasetsart University
- Wiroonsak Santipach, Kasetsart University
- Usana Tuntoolavest, Kasetsart University
- Thanaruk Teeramunkong, SIIT Thammasat University

Financial Chairs:
- Suneat Pranonsatit, Kasetsart University
- Itthisek Nilkhamheng, SIIT Thammasat University
- Teera Phatrapornnant, NECTEC

International Advisory:
- Akinori Nishihara, Tokyo Institute of Technology
- Nobuhiko Sugino, Tokyo Institute of Technology

Local Arrangement Chairs:
- Teerasit Kasetkasem, Kasetsart University
- Chalie Charoenlarpnopparut, SIIT Thammasat University

Publicity Chairs:
- Siriroj Sirisukprasert, Kasetsart University
- Waree Kongprawechnon, SIIT Thammasat University

Publication Chairs:
- Denchai Worasawate, Kasetsart University
- Miti Ruchanurucks, Kasetsart University
- Toshiaki Kondo, SIIT Thammasat University

General Secretary:
- Srijidtra Mahapakulchai , Kasetsart University

Supporting Organization:
- ECTI Association, Thailand
- IEEE Thailand Section

ORGANIZED BY

- Department of Electrical Engineering, Kasetsart University (http://www.ku.ac.th)
- Sirindhorn International Institute of Technology, Thammasat University (http://www.siit.tu.ac.th)
- National Electronics and Computer Technology Center, NSTDA (http://www.nectec.or.th)
- Tokyo Institute of Technology (http://www.titech.ac.jp)

ABOUT THE CONFERENCE

The International Conference on Information and Communication Technology for Embedded Systems (IC-ICTES 2011) is to provide an international forum for researchers and industry practitioners to share their new ideas, original research results and practical development experiences from all embedded system-related areas including ubiquitous computing, pervasive computing, embedded system design, development of new HW/SW-related theories and techniques in embedded systems, information and communication technology for supporting development of embedded systems, and information and communication technology used in embedded systems.

AREAS OF INTEREST

- **Embedded system architecture:**
  Multiprocessors, reconfigurable platforms, memory management support, communication, protocols, network-on-chip, real-time systems, embedded Microcontrollers
- **Real-time systems:**
  All real-time related aspects such as software, distributed real-time systems, real-time kernels, real-time OS, task scheduling, multitasking design.
- **Embedded hardware support:**
  System-on-a-chip, DSPs, hardware specification, synthesis, modeling, simulation and analysis at all levels for low power, power-aware, testable, reliable, verifiable systems, performance modeling, validation, security issues, real-time behavior and safety critical systems.
- **Embedded software:**
  Compilers, assemblers and cross assemblers, programming, memory management, object-oriented aspects, virtual machines, scheduling, concurrent software for SoCs, distributed/resource aware OS, OS and middleware support.
- **Hardware/software co-design:**
  Methodologies, test and debug strategies, real-time systems, specification and modeling, design representation, synthesis, partitioning, estimation, design space exploration beyond traditional hardware/software boundary and algorithms.
- **Testing techniques:**
  All aspects of testing, including design-for-test, test synthesis, built-in self-test, embedded test, for embedded and system-on-a-chip systems.
- **Application-specific processors and devices:**
  Network processors, real-time processor, media and signal processors, application specific hardware accelerators, reconfigurable processors, low power embedded processors, bio/fluidic processors, Bluetooth, hand-held devices, _ash memory chips.
- **Industrial practices and benchmark suites:**
  System design, processor design, software, tools, case studies, trends, emerging technologies, experience maintaining benchmark suites, representation, interchange format, tools, copyrights, maintenance, metrics.
- **Embedded computing education:**
  Curriculum issues, teaching tools and methods.
- **Emerging new topics:**
  New challenges for next generation embedded computing systems, arising from new technologies (e.g., nanotechnology), new applications (e.g., pervasive or ubiquitous computing, embedded internet tools) and new principle (e.g., embedded Engineering).
- **Embedded System Applications:**
  All ranges of applications on embedded system, including speech processing, image processing, network computing, distributed computing, parallel computing and power conversion.

CONFERENCE PUBLICATION AND PAPER SUBMISSION

Proceedings will be published by TAIST Tokyo Tech Program, National Science and Technology Development Agency (NSTDA). The first page should include the paper title, the names and the complete mailing addresses of all authors, and the e-mail address of the corresponding author. Each paper should consist of up to 200-word abstract, up to 5 keywords. No page number should be printed. All the text, figures and reference must be between 4-6 double-column A4 pages with font size of 10 pts. Authors MUST use IEEE manuscript submission guidelines (available at http://www.ieee.org/authors.html) for their initial submissions. All papers must be submitted electronically in PDF format only, using the conference management tool. The submitted papers must not be published or under consideration to be published elsewhere.

For further information, please contact

Srijidtra Mahapakulchai
Electrical Engineering Dept., Kasetsart University, 50 Phaholyothin Rd., Ladyao, Jatujak, Bangkok, Thailand, 10900. URL: http://www.icictes2011.org/
Phone : (662)942-8555 ext.1590, Fax : (662)942-8555 ext.1550 Email: secretary@icictes2011.org

Motor Imagery Classification Based on EEG Signal Using DWPT and Neural Network

Payat Jirasuwanpong[1], Miti Ruchanurucks[2], Chusak Thanawattano [3], Nobuhiko Sugino [4]

[1]*TAIST Tokyo Tech, ICTES Program*
email: payat.jira@gmail.com
[1,2]*Electrical Engineering, Kasetsart University, Bangkok, Thailand*
[3]*Biomedical Signal Processing Laboratory, National Electronics and Computer Technology Center, Pathumthani, Thailand*
[4]*Departure of Information Processing, Tokyo Institute of Technology, Tokyo, Japan*

Abstract— **The electroencephalogram (EEG) signal is one of the most well-known signals widely used in Brain Computer Interface system. This paper presents the new method of frequency decomposition in classification. Discrete Wavelet Packet Transform (DWPT) allows adjustable resolution of frequencies instead of Discrete Wavelet Transform (DWT), which decomposes the signal into a logarithmic frequency resolution. Subsequently, the Multilayer Percepton Neural Network (MLPNN) is used as a classifier in order to classify two of Motor Imagery (MI) tasks based on EEG signal. The results demonstrate the best accuracy of two-class (left and right hand motor imagery) classification is 65.56%.**

***Keywords*— BCIs, EEG, Motor Imagery, DWT, DWPT, MLPNNS**

I. INTRODUCTION

The classification of EEG patterns plays an important role in Brian-Computer Interface system (BCIs), which is an alternative channel to communicate between a human brain and computers. There are many applications for BCIs such as a computer cursor, computer graphic or a robotic limb. Electroencephalogram (EEG) is a non-invasive system, which records the signal from a human scalp. The system is easy to implement, but it has low signal-to-noise ratio. The brain waves recorded from a human scalp have small amplitude of approximately 100 μV. The frequency range of these brain waves from 0.5 to 100 Hz, and their characteristics are highly dependent on the degree of activity of the cerebral [1].

To increase performance of the BCIs, researchers have to understand the dynamics of brain oscillations better. In Motor Imagery, which is an imagination of movement, primary sensory and motor areas are activated [2]. The brain activity can be interpreted because brain activity associated with actual and imagined hand movement has similar topographies [3]. During motor imagery, sensorimotor activity changes the oscillatory patterns resulting in amplitude suppression called Event Related Desynchronization (ERD) or amplitude enhancement called Event Related Synchronization (ERS) on MU rhythm (7-13 Hz) and Beta rhythm (18-25 Hz) [1].

In this paper, we consider the time-frequency transform adjustable frequency resolutions. Although Discrete Wavelet Transform (DWT) has been used in many applications of Bio-signal processing [4] sometimes, it doesn't provide suitable frequency range. Owning to DWT, which produces good frequency localization at low frequencies and good time localization at high frequencies [5], the decomposed signals locate in sub-octave band. For solving this problem, Discrete Wavelet Packet Transform (DWPT) is used to extract wavelet coefficients from adaptable band. In DWPT [6], frequency range of each sub-band will be more specific than that of DWT. In the part of classification, The Multilayer Percepton Neural Network (MLPNN) is used as classifier, which is a powerful tool for pattern recognition [7].

In the second chapter, we explain EEG pre-processing, how to use DWPT to decompose the signal, and statistical models of feature extraction. Also, MLPNN is used as classifier trained by the Levenberg-Marquardt training algorithm. The third section presents results of the classification. Conclusions are given in the fourth section.

II. MATERIAL AND METHODS

A. Data description

The data of BCI competition 2003 is used to test our algorithm provided by Graz University of technology [8]. This data include three subjects: k3b, k6b, 11b. The recording was made with a 64-channel EEG amplifier from Neuroscan, using the left mastoid for reference and the right mastoid as ground. The EEG was sampled with 250 Hz, it was filter between 1 and 50 Hz with Notchfilter on. The subject sat in a comfortable chair with armrests. After trial begins, the first 2s were quite. t=2s an acoustic stimulus indicated the beginning of the trial, and a cross "+" is displayed. then from t=3s an arrow to the left, right, up or down was displayed for 1s; at the same time the subject was asked to imagine a left hand, right hand, tongue or foot movement, respectively, until the cross disappeared at t=7s.

B. Surface Laplacian Filtering

The raw EEG signals are spatially contaminated by the head volume conductor effect. The surface laplacian can be considered as a spatial high pass filter [9], which is necessary before further signal processing and feature extraction. It's similar to neighbourhood activity suppression by subtracting average adjacent channels. The finite difference implementation of surface laplacian was used, with the assumption that the distances from the channel of interest to its neighbouring channels are approximately equal.

$$V_j^{Lap} = V_j - \frac{1}{4}\sum_{k \in S_j} V_k \qquad (1)$$

Where V_j is the scalp potential EEG of the j^{th} channel and S_j is an index set of the neighbouring channels.

C. Discrete Wavelet Transform (DWT)

The wavelet transform decomposes a signal into a set of function obtained by shifting and dilating one signal function called mother wavelet. The decomposition of the signal leads to a set of coefficients called wavelet. All wavelet transform can be specified in terms of a low-pass filtering g.

$$G(z)G(z^{-1}) + G(-z)G(-z^{-1}) = 1 \qquad (2)$$

Where G(z) denotes the z-transform of the filtering g. It complementary high-pass filter can be defined as.

$$H(z) = zG(-z^{-1}) \qquad (3)$$

A sequence of filters with increasing length (indexed by i) can be obtained.

$$G_{i+1}(z) = G(z^{2i})G_i(z) \qquad (4)$$

$$H_{i+1}(z) = H(z^{2i})H_i(z) \qquad (5)$$

The normalized wavelet and scale basis functions $\varphi_{i,l}(k)$, $\psi_{i,l}(k)$ can be defined as

$$\varphi_{i,l}(k) = 2^{i/2} g_i(k - 2^i l) \qquad (6)$$

$$\psi_{i,l}(k) = 2^{i/2} h_i(k - 2^i l) \qquad (7)$$

where the factor $2^{i/2}$ is an inner product normalization, i and l are scale parameter and the translation parameter, respectively. Each stage consists of two down-samplers by two. h[.] is the discrete mother, high-pass filter. g[.] is its mirror version, low-pass filter. The down-sampled outputs of first high-pass and low-pass filters provide the detail, D and the approximation, A respectively. Other stages will be iteratively processed.

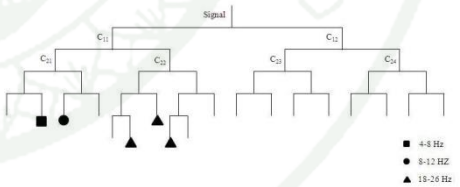

Figure 1. The structure of DWPT and the selected bands.

D. Discrete Wavelet Packet Transform (DWPT)

The classic wavelet transform will iteratively compute only approximation of a previous level. It means n levels of DWT performs n+1 sub-band signals (D_1, D_2, …, D_n, A_n). DWT has implemented by half cut off low-pass and high-pass filter, therefore DWT results in a logarithmic frequency resolution. DWPT allows a finer and adjustable resolution of frequencies. It gives a rich structure since DWPT iteratively processes both approximation and detail of a previous level shown in figure 1. The full DWPT n levels perform 2^n sub-band signals. For this reason,

DWPT has high frequency resolution. However, there is a computational complexity higher than that of classic DWT.

E. Feature extraction

Now that we have decomposed signals into Theta (4-7 Hz), MU (8-12 Hz) and Beta (18-25 Hz) [10] by retrieving coefficients of DWPT following in figure 1, the statistical features of each sub-band signal were used to represent the time-frequency distribution of EEG signal. The below features were extracted from the decomposed signals.

- Mean of the wavelet coefficients in each sub-band signal.
- Standard deviation of the wavelet coefficients in each sub-band signal.
- Energy of the wavelet coefficients in each sub-band signal.
- Ratio between wavelet coefficient energy and adjacent bands.

We have three dominant frequency bands (Theta, MU and Beta) and there are four statistical features of wavelet coefficient in each band. For motor imagery, three electrodes (C_3, C_z and C_4) were chosen to analyse EEG signal. Therefore, the original EEG signal was extracted to 36 dimension data (3×4×3 extracted feature vectors).

F. Artificial Neural Networks (ANNs)

Neural Networks have been successfully used in classification tasks. ANNs not only model the signal but also make a decision as to the class of signal. The advantage of ANN analysis over existing methods of biomedical signals analysis is that after an ANN has trained satisfactorily and the values of the weights and biases have been stored, testing and subsequent implementation is rapid. Multilayer Percepton Neural Networks (MLPNNs) are a nonparametric technique for performing a wide variety of detection and for estimating tasks. There are an input layer, a hidden layer and an output layer in MLPNN. In the hidden layer, each input x_i will be multiplied by adaptable weights w_{ji} after summing them the value passes though a function which can be a simple threshold or a sigmoidal function. Each weight w_{ji} is adjusted in order to reduce error E as rapidly as possible. The structure of a MLPNN classifier shows in figure 2.

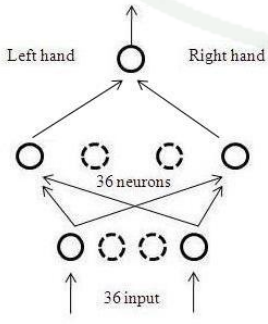

Figure 2. The structure of a MLPNN classifier with 36 feature inputs and 36 hidden neurons.

$$y_i = f\left(\sum w_{ji} x_i\right) \quad (8)$$

$$E = \frac{1}{2}\sum_j (y_{dj} - y_j)^2 \quad (9)$$

The MLPNN was trained by the Levenberg-Marquardt training algorithm [11], which solves some problems of the back propagation training algorithm.

III. Results

The EEG signal consists of multi-channel electrodes, which might be not relevant with motor imagery tasks. Therefore, the electrode sites C_3, C_z and C_4 were chosen as the signal and their four neighbourhoods were chosen for Surface Laplacian Filtering. The EEG signal is decomposed by DWPT, which performs specific frequency ranges. We retrieve wavelet coefficients from three different bands namely Theta (4-7 Hz), Mu (8-12 Hz) and Beta (18-25 Hz). Then, statistical models (mean, standard deviation, energy and ratio of energy with adjacent bands) of the coefficients in each sub-band are used as features to train the MLPNN classifier. In two-class classification (left and right hand motor imagery), we use "K3" data set which each class has 90 tasks divided into 45 tasks for training dataset and 45 tasks for testing dataset. To compare with previous methods DWT, selecting D1, D2, D3 and A3 sub-bands, and the MLPNN was implemented with the single hidden layered (36 hidden neurons). The MLPNN was used to classify the EEG signal based on a feature vector (36 inputs). The results show classification extracting from DWPT is more accurate than DWT and wavelet function Daubechies1 results in the best performance. Other results are shown in table1.

TABLE I. ACCURACY RATES OF THE TWO METHODS USING VARIOUS WAVELET FUNCTIONS.

Wavelet	Methods of decomposition	
	DWT	DWPT
haar	58.89%	56.67%
db1	61.11%	65.56%
db2	54.44%	61.11%
db4	53.33%	60%
db6	48.89%	63.33%

IV. CONCLUSION

In this paper, the Discrete Wavelet Packet Transform (DWPT) is proposed to improve accuracy of classification instead of the Discrete Wavelet Transform (DWT). For brain-computer interface system, we must choose the method that is reliable and fast enough. The MLPNN used for the classification of EEG signals is trained by extracted features from the statistical DWPT coefficients. It's found that DWPT with Daubechies1 wavelet function give the highest accuracy. Therefore, the DWPT technique, which provides specific frequency ranges, has accuracy and performance of classification higher than that of the DWT technique.

V. ACKNOWLEDGEMENT

This research is financially supported by Thailand Advanced Institute of Science and Technology (TAIST), National Science and Technology Development Agency (NSTDA), Tokyo Institute of Technology and Kasetsart University (KU). Authors would to thank NTC Telecommunication Research Laboratory at Department of Electrical Engineering, Kasetsart University for Matlab program.

REFERENCES

[1] Maan M. Shaker, "EEG Waves Classifier using Wavelet Transform and Fourier Transform," International Journal of Biological and Life Sciences 1:2 2005.

[2] Chris Neuper, Reinhold Scherer, Miriam Reiner, Gert Pfurtsheller, "Imagery of motor action; Differential effects of kinesthetic and visual-motor mode of imagery in single-trial EEG," Cognitive Brain Research 25 (2005) 668-677.

[3] Dennis J. McFarland, Laurie A. Miner, Theresa M. Vaughan, Jonathan R. Wolpaw, "MU and Beta Rhythm Topographies during Motor Imagery and Actual Movements," Brain Topography, Volume 12, Number 3, 2000. J. Clerk Maxwell, A Treatise on Electricity and Magnetism, 3rd ed., vol. 2. Oxford: Clarendon, 1892, pp.68–73.

[4] Neep Hazarika, Jean Zhu Chen, Ah Chung Tsoi, Alex Sergejew, "Classification of EEG signals using the wavelet transform," Signal Processing 59 (1997) 61-72.

[5] Abdulhamit Subusi, "EEG signal classification using wavelet feature extraction and a mixture of expert model," Expert System with Applications 32, 2007, 1084-1093.

[6] S. Zhang, C. Zhu, J. K. O. Sin, and P. K. T. Mok, "A novel ultrathin elevated channel low-temperature poly-Si TFT," *IEEE Electron Device Lett.*, vol. 20, pp. 569–571, Nov. 1999.

[7] Changmok Oh, Min-Soeng Kim, Ju-Jang Lee, "EEG signal classification based on PCA and NN," SICE-ICASE International Joint Conference 2006.

[8] Gert Pfurtscheller, Alois Schlögl. (2003), BCI competition 2003, Available: http://www.bbci.de/competition/iii/#datasets

[9] Tao Wang, Jie Deng, Bin He, "Classifying EEG-based motor imagery tasks by means of time-frequency synthesized spatial patterns," Clinical Neurophysiology 115 (2004) 2744-2753.

[10] Zhendong Mu, Dan Xiao, Jianfeng Hu, "Classification of Motor Imagery EEG Signal Based on Time-frequency Analysis," International Journal of Digital Content Technology and its Applications Volume 3, Number 4, 2009.

[11] K. Madsen, H.B. Nielsen, O. Tingleff, "METHODS FOR NON-LINEAR LEAST SQUARES PROBLEMS," Informatics and Mathematical Modeling Technical University of Denmark, 2004

CIRRICULUM VITAE

NAME : Mr. Payat Jirasuwanpong

BIRTH DATE : August 3, 1987

BIRTH PLACE : Bangkok, Thailand

EDUCATION :

YEAR	**INSTITUTE**	**DEGREE/DIPLOMA**
2008	Kasetsart Univ.	B.Eng. (Electrical Engineering)
2011	Kasetsart Univ.	M.Eng. (Information and Communication Technology for Embedded Systems)

POSITION/TITLE : -

WORK PLACE : -

SCHOLARSHIP/AWARDS : TAIST ICTES Master Degree Scholarship

PUBLICATION : ICICTES 2011